Norwegian University of
Science and Technology

Fabrication of Cellular Microarrays

Aurora Resell

Chemical Engineering and Biotechnology
Submission date: June 2017
Supervisor: Marit Sletmoen, IBT

Norwegian University of Science and Technology
Department of Biotechnology and Food Science

Fabrication of Cellular Microarrays

Aurora Resell

June 28, 2017

Preface

The work for this master thesis was carried out at the Department of Biotechnology at the Norwegian University of Science and Technology (NTNU) in Trondheim, during the spring term of 2017. A large part of the work was carried out at NTNU's nanolab.

I would like to thank my supervisor Marit Sletmoen for guidance and encouragement during the project.

I would also like to thank the staff at nanolab for always being helpful.
Additionally, I would like to thank my fellow master students working on this project for always staying positive and wishing to find solutions throughout the laboratory work.

Abstract

Cellular microarrays are known for their use as a tool to investigate variations between single cells in terms of how they respond to different physiological parameters. The work of this thesis focused on developing a procedure for fabricating such cellular microarrays, which was mainly done by investigating the effects of the experimental parameters in the photolithography step.

Factors such as homogeneity of the photoresist layer and exposure doses of UV-light proved to be crucial for the final result of the microarrays. The photoresist used during photolithography, SU8, brought several challenges as the resist layer was inhomogeneous and often cracked. The inhomogeneities in the resist layer resulted in PDMS stamps with non-optimal features, causing difficulties during microcontact printing.

Fluorescently labeled PLL and quantum dots were used for investigating whether or not the PDMS stamps made were suited for microcontact printing. Yeast cells were attempted immobilized onto glass surfaces microcontact printed with PLL. The PLL attached poorly to the glass surfaces when cells were added.

Sammendrag

Cellulære microarrays er nyttige redskap for å undersøke variasjoner mellom hvordan celler responderer på forsjellige fysiologiske parametere. I dette arbeidet ble det fokusert på å utvikle en metode for å lage slike microarrays, hovedsaklig ved å undersøke effekten av ulike parametere i fotolitografidelen av produksjonen.

Homogeniteten av fotoresistlaget og mengden UV-lys under eksponering viste seg å være svært viktige faktorer for for de endelige microarrayene. Den benyttede fotoresisten, SU8, kom med flere utfordringer. Fotoreistlaget var ofte uhomogent og hadde en tendens til å sprekke. Ujenvnheter i fotoresistlaget gav PDMS-stempel hvor mønsteret var av lav kvalitet, noe som gjorde microkontaktprintingen utfordrende.

PLL merket med fluorescens og kvanteprikker ble brukt for å undersøke om PDMS-stempelene var brukbare for mikrokontaktprinting. I tillegg ble gjærceller forsøkt immobilisert på glassoverflater stemplet med umerket PLL. Ved tilsats av gjærceller til glassoverflatene ville ikke PLL forbli festet til overflaten.

Symbols and Abbreviations

AFM	Atomic Force Microscopy
BSA	Bovine serum albumin
FITC	Fluorescein isothiocyanate
IPA	Isopropyl alcohol
IFY	Department of physics NTNU
kDa	Kilodaltons
M	Molar [mol/L]
MOPS	3-(N-morpholino)propanesulfonic acid
MQ	Milli Q
M_w	Molecular weight
NTNU	Norwegian University of Science and Technology
PD	Polydopamine
PDMS	Polydimethylsiloxane
PEB	Post exposure bake
PEG	Polyethylene glycol
PEI	Polyethylenimine
PLL	Poly-L-Lysine
PVA	Polyvinyl alcohol
QD	Quantum Dots
Rpm	Rotations per minute
SAM	Self assembled monolayers
YPD	Yeast extract peptone dextrose
λ	Wavelength
μCP	Microcontact printing

Contents

1 Introduction **1**
1.1 Background . . . 1
1.2 Cellular microarrays . . . 3
1.2.1 Photolithography . . . 5
1.2.2 PDMS . . . 10
1.2.3 Stamping by μCP . . . 12
1.3 Chemicals and cells useful in PDMS-stamp investigation . . . 14
1.3.1 Quantum dots . . . 14
1.3.2 PLL . . . 14
1.3.3 Yeast . . . 15
1.3.4 Polystyrene beads . . . 16
1.4 Imaging methods . . . 16
1.4.1 Bright field microscopy . . . 16
1.4.2 Phase contrast microscopy . . . 16
1.4.3 Fluorescence microscopy . . . 16
1.4.4 Atomic force microscopy . . . 18
1.5 Aim of the project . . . 19

2 Materials and methods **20**
2.1 Stamp production . . . 20
2.1.1 Master mold . . . 20
2.1.2 PDMS replica molding . . . 22
2.2 Studying PDMS stamps . . . 22
2.2.1 Imaging of PDMS stamp . . . 22
2.3 Microcontact printing (μCP) . . . 22
2.3.1 Printing quantum dots . . . 22
2.3.2 Printing PLL-FITC and PLL . . . 23
2.4 Immobilisation of yeast cells . . . 23
2.4.1 Yeast cell inoculation . . . 23
2.4.2 Immobilisation on stamped surface . . . 24
2.5 Immobilisation of polystyrene beads . . . 24
2.6 Investigation of PDMS stamps by AFM . . . 24

3 Results **25**
3.1 Resist thickness . . . 25
3.2 Imaging of master molds . . . 26
3.3 Imaging of PDMS stamps . . . 29
3.4 μCP . . . 33
3.4.1 Printing quantum dots . . . 33

3.4.2 Printing PLL-FITC 35
3.4.3 Immobilization on functionalized surfaces 41
3.5 Investigation of PDMS stamps by AFM 44

4 Discussion **51**
4.1 Effect of photolithography parameters 51
4.1.1 Resist homogeneity 51
4.1.2 Exposure doses 54
4.2 Effect of PDMS stamp quality on μCP 54
4.3 Immobilization 57
4.4 Quality of results 59
4.5 Future work 59

5 Conclusion **60**

Appendices **68**

A Edge bead measurements **i**

1 Introduction

1.1 Background

Immobilization of cells by attachment onto a supporting material in a specific pattern, known as cellular microarrays, have proven to be useful for several purposes. Cellular micorarrays allows investigation of the cell-to-cell variations in physiological parameters such as stress-resistance, growth rate, or the triggering of a cellular response such as a specific secreted factor. Cellular microarrays make it possible to make measurements on single cells rather than entire populations. As variations in cellular sub-populations from the overall population average may cause an effect on the populations response to disturbance, it is of importance to investigate the heterogeneity of the cell-population. This type of information is useful when understanding for example microbes causing infections and microbes in soil and water.[1][2]

Phenotypic variations persistent for more than one generation are known to occur in bacterial populations even though there is no direct change in in the DNA-sequence of the bacteria. These types of variations are generated by non-genetic mechanisms. An important case of phenotypic variation is bacterial persistence, which means that a genetically identical bacterial population responds heterogeneously to antibiotics. The bacteria able to escape the effects of antibiotics are called persisters, they make up a subpopulation very tolerant to antibiotics without undergoing genetic change.
Bacterial persistence is important when studying the dynamics of population variability.[3][4]

Persister cells are not to be confused with resistant cells, cells which are able to grow in the presence of antibiotics, as the persister cells are *not* able to grow in the presence of antibiotics. Additionally, resistance is acquired genetically and passed on to the next bacterial generations, whereas persister cells have not gone through any change in their genetic material.
Persister cell subpopulations make up a small part of the cells in the exponential phase of a colony, while in the stationary phase and in biofims they make up a significant fraction. It is suggested that persister cells persist by taking a dormant state where the cells are metabolically inactive. Chronic infections may be due to such cells as the population regrows after antibiotic treatment thanks to the persister cells. The regrown population will still be sensitive to the antibiotics. This is of relevance in for instance tuberculosis treatment where a sole, surviving bacteria is able to re-start an infection. [3]-[9]

Often infections occur on implants such as catheters, caused by biofilm formation. This could be coupled to persister cells which are being shielded from the immune-system by the biofilm's exopolymer matrix.[10][11]
Many bacteria form biofilms. Here, spatial segregation of the bacteria is important for the bacteria's development on a cellular and communal level.[12]

Persistence is not the only possible outcome from heterogeneity in gene expression. Events connected to variability in phenotypes also occur; for example bistability where cells go into either one or the other phenotype causing two distinct subpopulations. Traditionally it was thought that all cells in in a bacterial population would express genes in a relatively uniform way under certain conditions, but bistability shows that this is not necessarily the case. A bi-stable bacterial population has for example the ability to shift between utilizing or not utilizing a specific nutrient depending on its availability.[13]-[15]

Differences in phenotypes among genetically identical cells provide flexibility when it comes to adapting to a varying environment as well as leading to division of labour among the cells letting the population grow at a higher rate.[16][17] In order to measure phenotypic heterogeneity, comparisons between many individual cells or following individual cells over time is necessary.[16][17] Some methods investigated are fluorescent proteins used as gene reporters combined with microscopy or flow cytometry.[17]-[19] Flow cytometry works by passing particles in a fluid through a laser. The components of the cells are labeled with fluorescence and are excited by the laser causing emission of light at various wavelengths, which gives information on chemical and physical characteristics. However, flow cytomerty is not able to track a cell over time.[20] For imaging live cells time lapse fluorescence microscopy is an approriate tool. It allows investigation of cellular processes and events over time, giving good temporal and spatial distribution.[21]

Tools such as bacterial microarrays allows individual manipulation of cells and their extracellular environment, making changes in the way microbial physiology and behaviour is studied. By using soft lithography it is possible to study single microbes in a cost-efficient and simple way.[22]

1.2 Cellular microarrays

Microarray tools have been adapted to several types of biomolecules and biological samples such as DNA, proteins tissue and cells.[23] DNA Microarrays are usually defined as small, solid supports to which genes or portions of genes are affixed and arrayed spatially in a known pattern, often termed "gene chips". These arrays are used for finding patterns of gene expression by RNA-DNA hybridization. Parts of known single-stranded nucleic acids, nucleic acid probes, are used for the hybridization. The probes are labeled radioactively or with fluorescence. RNA from cells grown under certain conditions hybridizes with the DNA-segments attached to the solid support before scanning and analyzing.[24] In order to obtain information on the proteins the genes of interest encode, protein chips are used. Interactions of the proteins, their targets and substrates are possible to identify using protein chips, additionally the chip is useful for diagnostics.[25] Microarray techniques have been applied for analysis of tissue samples as well, being highly useful in cancer research.[26] Living-cell microarrays have been developed with the intention to screen genomic and chemical libraries and to investigate local cellular micro-environments, being able to identify the relationship between cells and their local surroundings.[27]

All arrays rely on almost the same principle; a group of specific reactive molecules is immobilized onto a solid surface and exposed to a mixture to be analyzed. By various detection approaches, such as fluorescence, identification of the sites where recognition has occurred is possible. Application of arrays is being developed for application within biology, medicine and toxicology. Arrays where DNA, RNA and proteins are used have the benefit of high specificity for the recognition events. When live cells rather than molecules are being used in arrays much of the specificity is gone, but this loss is compensated for by the ability to directly study biological effects on living systems. Live cell-arrays was at first intended to be a useful tool for studying gene expression, but shows promise for a large variety of applications.[28][29] When the techniques for preparing, preserving and understanding such arrays are improved, they are thought to be an efficient analytical tool on the same level as DNA microarrays.[30]

In the following section there will be focused on strategies for the immobilization of live bacteria or yeast cells in ordered and predefined patterns on a glass surface. Preparation of such microarrays of bacteria or yeast cells could be done by different strategies. The main two approaches are either depositing the cells directly onto a substrate in a defined pattern or using

surface patterning techniques that causes the cells to only attach to specific areas in a certain pattern. For the first type of approach the array is made by depositing droplets with the suspended microorganisms, causing limitations with respect to the droplet size among other challenges.[31][32] The second type of approach have the advantage of needing less direct handling of the cells. A surface, for instance a glass slide, is pattered with either a chemical or a topographic pattern in micro scale.
Examples of topographical patterns where bacterial or yeast microarrays successfully have been created are by using pillars within bacterial size ranges and by holed arrays in a silicon structure.[12][33][34] Although these methods have generated good results, they require a lot of time and clean-room access.
By μCP chemical patterning is obtained. It is demonstrated that μCP is an effective tool for functionalizing surfaces with specific chemicals. It has been especially useful for biological applications.[35] By μCP it is possible to form self-assembled monolayers, SAMs, with areas restricted by different physical and chemical properties in patterns.[36] It is a simple and cost-efficient method for patterning surfaces with a high degree of adaptability and accuracy down to sub-micrometer scales. The newest techniques make μCP a reproducible way of patterning with high resolution. Stamps used for microcontact printing are prepared by the use of photolithography and soft lithography.[37]

In figure 1.1 an example of a bacterial microarray produced by the use of μCP is illustrated. *P. putida* immobilized on arrays of PD-islands on a glass-surface deactivated by PEG is shown.

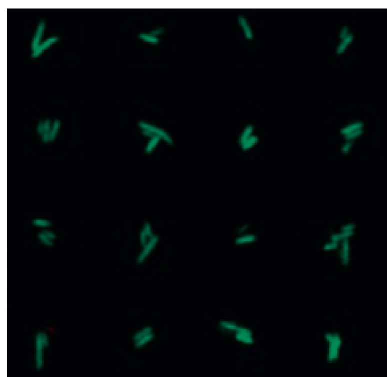

Figure 1.1: *P. putida* imobilized on PD-islands on PEG-covered glass-surface stained with fluorescence, performed by using stamping by μCP. Figure taken from [38].

1.2.1 Photolithography

The process of transferring a specially designed pattern from a mask onto a layer of photoresist on the surface of a wafer is known as photolithography. The mask used for this purpose is called a photo-mask and is composed of an opaque plate, made from for example quartz or glass, with transparent regions in a defined pattern where light is let through. The technique was initially developed for production of printed circuit boards, being very important for the semiconductor industry.[39][38][40]

Photoresists

A photoresist is a material sensitive to lights of certain wavelengths, mainly UV-light. The wafer, often 2-4 inches in diameter made of silicon, is coated with photoresist before being exposed to UV-light through a photo-mask, making a pattern in the photoresist-coat. Laboratory areas were photolithography is performed often have yellow lighting, as most photoresists are insensitive toward this type of light. Polymers, solvents, additives and sensitizers are the basic ingredients of a photoresist. Before the resist is spun onto the wafer solvents can make up as much as 75% of the mixture. Photoresists are split into two different categories; negative and positive. In a positive type of photoresist polymerization and crosslinking occurs before the resist is exposed to UV-light. Following exposure, the parts of the positive photoresist being exposed turn into a state where it is soluble and will dissolve in the developer. The resulting pattern will be equivalent to the pattern of the mask. By using positive photoresist it is obtained patterns of higher resolution in the nanometer-scale than for negative resists. Negative photoresists work in an opposite manner. Only the parts of the resist exposed to UV-light will polymerize and crosslink. These parts will stay hardened on the surface of the wafer following development, while the unexposed parts are dissolved. The resulting pattern for this case will be reversed of the pattern on the mask. The result of exposing a positive and a negative photoresist to UV-light is illustratd in figure 1.2. The reaction taking place in the positive photoresist is named photo-solubilization, while the one taking place in the negative photoresist is called an aphotochemical reaction. The polymer in the photoresist is an organic compound, often with advanced ring- and chain-formations. The polymer is the component in the photoresist which binds to the surface of the wafer.[41]

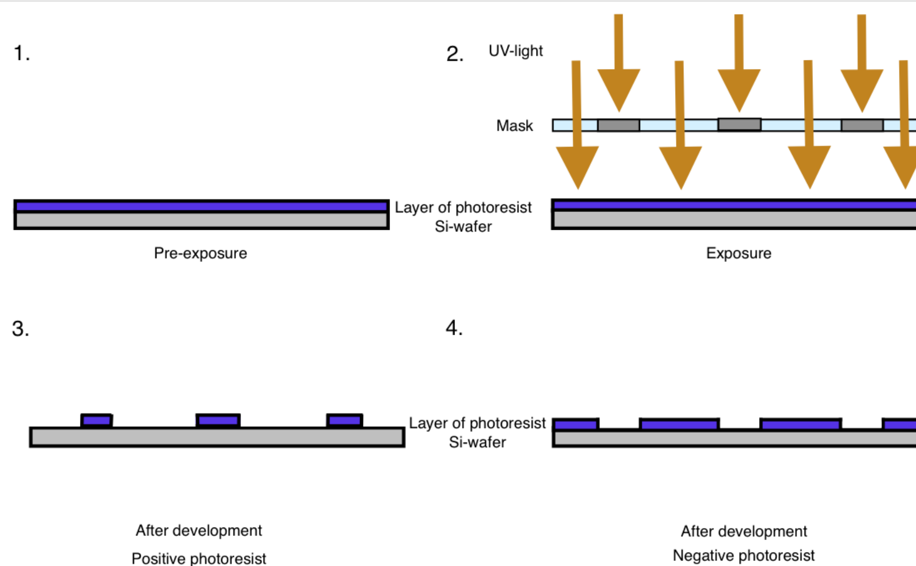

Figure 1.2: The difference between a positive and a negative photoresist spread onto a Si-wafer after exposure to UV-light through a photo-mask and after development. For the positive photoresist polymerization and cross-linking happens before exposure. The parts of the resist exposed to UV-light dissolves, as seen from 3. in the figure. In a negative photoresist only the parts exposed to UV-light cross-links and polymerizes, as seen from 4. in the figure. During the actual exposure performed in a laboratory, there is no space between the mask and the photoresist. Adapted from[41].

SU-8 Photoresist

One commonly used negative type of photoresist is SU-8. It is used where a thick, chemically stable pattern is wanted. The resist is of epoxy type. SU-8 has proven to be highly sensitive towards changes in process-parameters, such as exposure dose and post exposure bake.[42][43] The name SU-8 comes from the structure of the average SU-8 molecule which contains eight epoxy groups. This structure is shown in figure 1.3. The resulting structure after exposure to UV-light is highly crosslinked, causing it to have good chemical and thermal stability. SU-8 resists are acid catalyzed, meaning that acid is produced upon UV-light exposure. This acid acts as a catalyst for the reaction taking place during the post exposure bake.

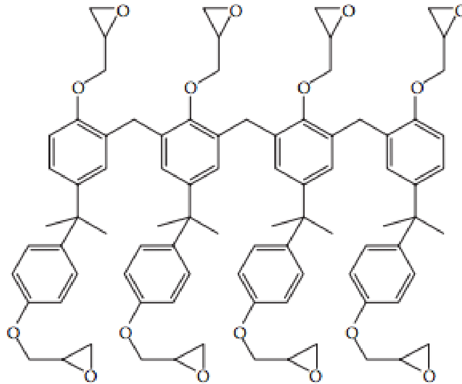

Figure 1.3: The chemical structure of the average epoxy-molecule in SU-8 resists. These molecules are the ones crosslinking upon UV-light exposure.[44]

The many epoxy groups in SU-8 resist is beneficial for the adhesion of the resist to the substrate, for instance to the surface of an Si-wafer. However, there are some challenges related to the use of SU-8. Differences in thermal properties between the resist and the substrate are quite common, and may cause stress leading to cracking of the photoresist layer or disfiguring of the side walls in the pattern. This can happen during the baking steps in SU-8 photolithography.[44]

Spin coating

The three main operations of photolithography are coating of photoresist, exposure and development. Additionally there are several steps involving baking and chilling in order to obtain the highest possible resolution. Additionally, the substrate must be cleaned before the operations begin. Spin coating is performed by applying the liquid photoresist onto the substrate, such as a wafer, before spinning it in order to get a thin, homogeneous coat. Centrifugal forces from the rotation makes the resist spread all over the wafer. The thickness of the resist-layer obtained after spinning is dependent on the viscosity of the photoresist and the spin rate. With a higher spin rate, the layer becomes thinner and more homogeneous, while a higher viscosity causes a thicker layer. The solvents evaporate quickly from the resist when being spun, meaning that the viscosity of the resist changes. This is why it is necessary to raise the spin speed rapidly before the properties of the resist changes. After spin coating is completed there is often a thicker layer of photoresist near the edges, known as edge beads. Edge beads makes it difficult to achieve sufficient contact between the mask and the photoresist during exposure, causing a lower resolution of the features in the resist.[41][45][46] This is illustrated in figure 1.4. For the various types of SU-8 photoresists typical

spin-coating parameters are acceleration speed between 200-500 rpm/s and spin speeds ranging between 1000-4000 rpm. The time of spinning varies from a few seconds up to several minutes. [44]

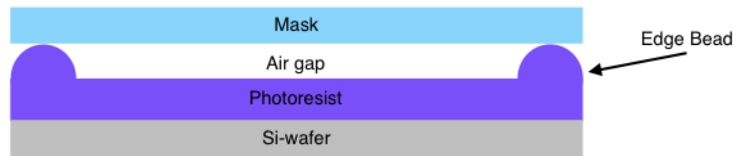

Figure 1.4: The formation of an edge bead following spin coating leads to insufficient contact between the resist and the mask. This will in turn lead to a lower resolution of the pattern on the resist layer.

Edge beads can be removed manually with solvent appropriate for the resist used. Several spin-coaters have built-in edge bead removal systems.

Other issues related to spin coating is the formation of comet-like stripes in the resist and the appearance of bubbles. Such irregularities are the beginning of defects in the final resist pattern. Bubbles of air could appear in the resist during refilling of when it is dispensed onto the substrate. N_2-bubbles appear due to continuous decomposition of the photo-active compound in the resist. Outgassing of the resist before spin coating could decrease the amount of bubbles. Inadequate cleaning of the substrate prior to spin-coating or expiration of the resist is the reason of particles in the resist layer. Bubbles and particles is the source of comet-like stripes in the resist as they are forced towards the edge when the substrate is spun.[47][48]

Soft baking

In order for solvent to evaporate from the resist layer a soft bake is performed after the spin-coating step. In addition, soft baking is beneficial for adhesion of photoresist to substrate. For several types of photoresist, including SU-8, soft bake is done by placing the coated substrate on a hotplate. This allows good control of the temperature, which is important to avoid cracking. Often the temperature is ramped up in a controlled manner. It is proven that including this step results in higher resolution of the pattern. However, exaggerated baking will cause a higher frequency of cracking. The time and temperature needed for soft baking depends on the solvent content of the resist and the thickness of the resist layer. The thicker resist layer, the more difficult of the solvent to evaporate.[42][44][49]

Exposure
The experimental parameters during exposure in a photolithography process need to be optimized in order to achieve the best possible transfer of the pattern of the photo-masks onto the resist layer. When SU-8 resist is used UV-light in the the range of 350-400 nm is favorable. The exposure dose is given by the following equation.

$$Light\ intensity\ [W/cm^3] \times Exposure\ time\ [s] = Exposure\ dose\ [J/cm^2]$$

Usually the light intensity is fixed, meaning that changing the exposure dose is done by varying the exposure time. Non-optimal exposure doses cause either under- or over- exposure of the resist. Underexposure will result in dissolution of the pattern or make the resist layer come off the substrate while developing. In SU-8 resist his happens due to insufficient polymerization of the resist throughout the entire layer. Overexposure of the resist leads to occurrence of T-topping and to expansion of the pattern. T-topping is defined as what happens when UV-light with $\lambda < 350$ nm is absorbed on the surface of an SU-8 resist. This causes formation of acid which diffuses to the sides, leading to polymerization of a thin photoresist layer.[44][42]

Post exposure bake
Following exposure the substrate covered with a layer of resist is heated, known as post exposure bake (PEB). By applying heat, the process of cross-linking the polymer matrix is activated further. This step is necessary to complete polymerization of the resist layer. The properties of the pattern will depend on the settings during PEB. Here, as for the soft bake, the maximum baking temperature is reached step-wise in order to reduce stress. If the PEB is carried out at insufficient temperatures or time periods, the cross linking will not be complete, which could cause the resist layer to be damaged in the developing step. If the thermal stress is too high cracking, bending or loosening of the resist layer could take place. The risk of high thermal stress increases with the resist layer's thickness.[44]

Development
The resist-covered substrate is immersed in developer, dissolving parts of the resist based on its final chemical structure. For this to work as intended, the solubilities of the exposed parts and the non-exposed parts of the resist should be very different in the type of developer used. For SU-8 the unexposed, un-polymerized parts of the resist layer will dissolve in the developer. As for the other steps in photolithography, the thickness of the resist decides the

parameters. For a substrate with a relatively thin layer, <10 μm, developing will take a few minutes, while for thicker layers, > 400 μm, the developing time can be as much as several hours. The substrate needs to be agitated during development, something which is usually done manually. Agitation is necessary for keeping a flow of fresh developer to the patterns in the resist layers, although exaggerated agitation may cause certain patterns to suffer mechanical damage. During drying static friction forces could cause bending and joining of parts of the pattern for SU-8 resists. A typical way of lowering the forces is by rinsing with IPA during the drying step. After development a relief topography which may serve as either a structural element or a mold for further processes is complete.[44][40] Formation of a white film on top of the resist while rinsing indicates underdevelopment of the substrate.[42] Another baking step may be carried out after the development depending on the further intended use of the pattered substrate.

The finished product, often an Si-wafer as substrate, with a patterned photoresist layer on top is called the *master mold* in μCP processes.

1.2.2 PDMS

When a wafer with a photoresist pattern, the master mold, is finished the next step in the stamp production takes place. The stamps intended for μCP printing are usuallly made out of PDMS, polymethylsiloxane, due to its suitability. PDMS is a silicon rubber displaying highly stable physical and chemical properties. The chemical structure of PDMS is shown in figure 1.5

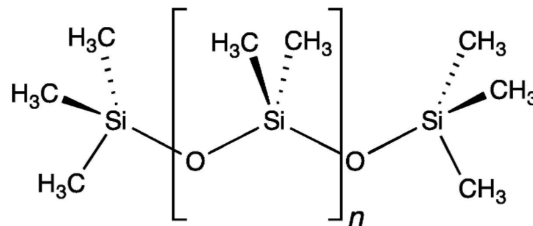

Figure 1.5: Chemical structure of the PDMS molecule.

The flexibility of the PDMS allows the stamp to achieve good, consistent contact with various surfaces. The PDMS is still rigid enough to stamp patterns with features down to micro- and even nano- meter precision. Another positive feature of PDMS stamps are their transparency. This is of great advantage in for example microscopy applications. Use of PDMS in stamp production is relatively cheap, fast and available.[48][50] Figure 1.6 illustrates

the PDMS poured over a master and the cured PDMS stamp removed from the master. If a master of good quality is available, PDMS-molding is an efficient way of producing stamps for use in μCP.

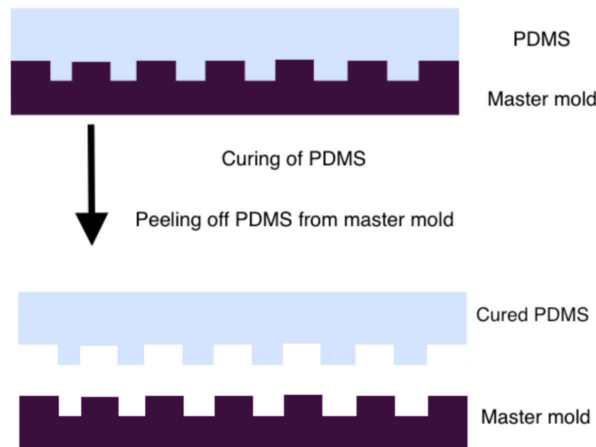

Figure 1.6: PDMS poured over a master with the desired pattern. When the liquid ingredients are well blended, the mixture will cure into a flexible elastomer. Curing is usually carried out at elevated temperatures After the PDMS is cured the stamp is removed from the master. One single master can be used to produce several PDMS stamps, as long as the master stays intact.[35][51]

However, there are some restrictions and complications related to the use of PDMS. Residues of pre-polymer and PDMS of low M_w may be present in the cured stamp and is prone to leaching from the stamp when μCP. This causes errors in the printing.[52] When patterns with features in the sub-micrometer range are attempted stamped, the features has the habit of collapsing. This happens due to the flexibility of the PDMS stamp. Other types of stamp deformities include buckling, sidewall collapse and lateral collapse.[37][48][53] In addition to collapsing features, PDMS stamps are restricted by their hydrophobic character. Polar molecules are consequently repelled from the stamp surface, causing insufficient inking and thus a non-satisfactory stamping onto the desired substrate. Another consequence of the hydrophobicity of the surface is denaturation of proteins when they are applied to the stamp. The stamp surface can be modified into being more hydrophilic by for example oxygen plasma treatment. This type of treatment creates radical sites on the stamp surface, leaving it hydrophilic. However, the plasma treatment is not permanent.[48][54]

Whether or not a PDMS stamp exhibits deformation during stamping is dependent on the aspect ratios of the features. The aspect ratio is defined as the feature's height divided by the lateral dimensions of the features.

Buckling and lateral collapse of the features are caused by a high aspect ratio, while roof collapsing is caused by low aspect ratios. Some of the various possible deformations of a PDMS stamp during μCP is illustrated in figure 1.7.[37][55]

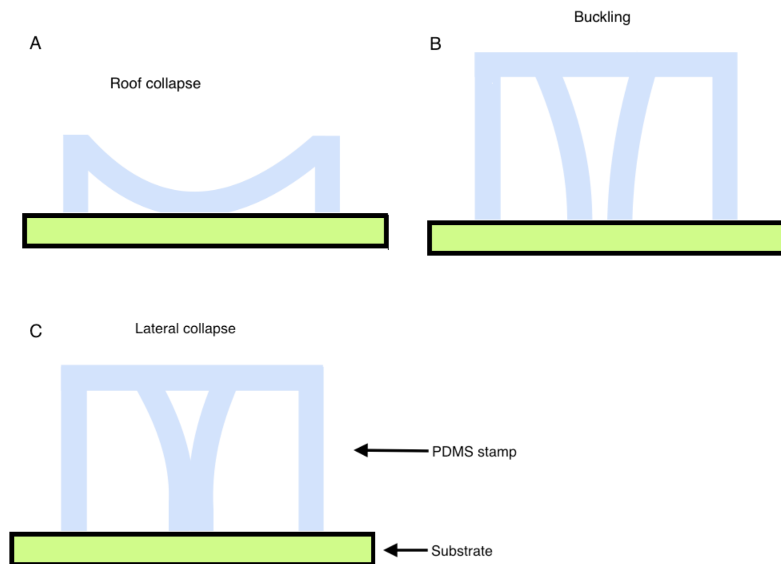

Figure 1.7: Some of the various deformation of PDMS stamps which may occur during μCP. Part A of the figure shows roof collapse, a type of deformation associated with low aspect ratios; the height is much smaller than the lateral dimensions of the stamp. Part B and C of the figure shows deformations associated with high aspect ratios; the height is large relative to the lateral dimensions. Deformation decreases the reproducibility of the pattern printed on the substrate surface. Adapted from [37] and [53].

Other occurrences that alters the reproducibility of the pattern is shrinking and swelling of the PDMS stamp. When PDMS is cured it shrinks approximately by 1 percent. Several non-polar organic solvents causes the stamp to swell.[37][56] Diffusion of ink laterally along the substrate during stamping is also a challenge.[37]

1.2.3 Stamping by μCP

Microcontact printing, μCP, uses the relief pattern of the PDMS stamp to from SAMs on a substrate surface upon contact. The method can be compared to ordinary printing, it includes a stamp, ink and a substrate surface.[48][56] The components of and a common way to perform μCP is presented in figure 1.8.

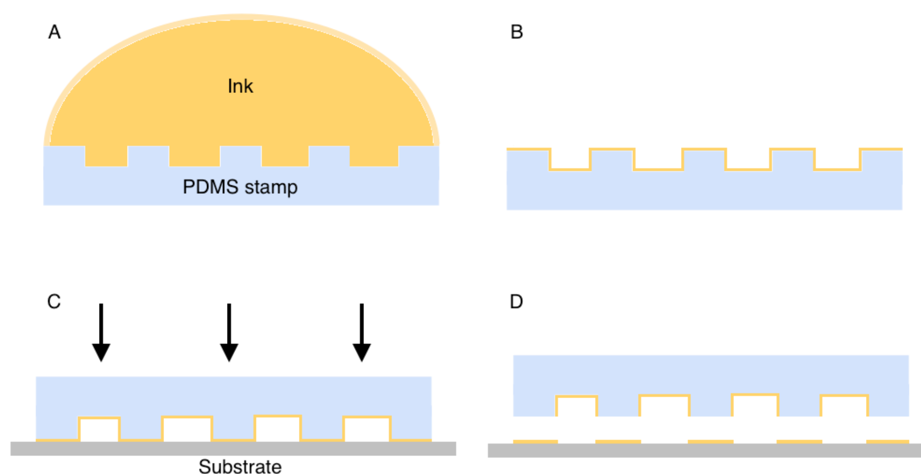

Figure 1.8: Illustration of how a PDMS stamp is used for μCP. Part A of the figure shows the stamp covered by an ink of interest. In part B the excess ink is removed and the PDMS is ready to be stamped. Part C shows the stamping of the ink onto the surface. Often, but not always, pressure is applied to the stamp in order to achieve sufficient contact between the pattern of the stamp and the surface. In part D a successful transfer of the ink in the stamps pattern on the substrate is displayed.

When the method of μCP using PDMS stamps first was developed, it was used for printing SAMs onto gold.[57] The ways of functionalizing a surface with a specific chemical by the application of a pattered PDMS stamp is useful for several applications, especially biological applications.[35] As discussed in 1.2, μCP is used for preparation of bacterial microarrays. The advantage of bacterial microarrays is the possibility to better investigate cell-substrate interactions, allowing discoveries not achievable with conventional culturing approaches.[35] In addition to bacterial microarrays, μCP makes fabrication of protein arrays and DNA arrays possible. μCP of proteins onto glass have been carried out by using PLL-solutions as ink. Due to the non-polarity of the PDMS surface and the positively charged nature of the PLL molecules, plasma treatment of the stamp helped the PLL bind reversibly to the now hydrophilic surface of the stamp.[35][58] A challenge in μCP of proteins is that a conformational change of the proteins occur when they absorb to the stamp. This makes it necessary for the substrate to hold properties more in favor of the transfer of proteins than the PDMS.[59][60] DNA arrays are prepared by μCP. DNA pieces the size of 20- 1600 base pairs have been stamped with μm precision. This method reduced the time and amount of DNA needed for various analysis.[61][62]

1.3 Chemicals and cells useful in PDMS-stamp investigation

1.3.1 Quantum dots

Quantum dots, QDs, are small semiconducting particles with a size of 2-10 nm. One of their most advantageous features is their fluorescent character, which is significant for several optical applications.[63][64] It is possible to functionalize QDs, depending on their intended use. An example is functionalization with carboxylate groups which is use for for coupling to amine groups.[65]

1.3.2 PLL

Poly-L-lysine, PLL, is one of the polylysine stereoisomers, it is a positively charged, bio-compatible amino acid polymer. The structure is given in figure 1.9.

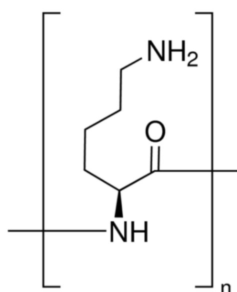

Figure 1.9: Structure of the poly-L-lysine molecule.[66]

By treating a surface, for example glass or plastic, with polylysine cell-adhesion to the surface is made possible. This adhesion is explained by the negatively charged surfaces of the cells and the positively charged layer made up from adsorbed polylysine. Cells attached to polylysine treated surfaces serves many experimental applications. Other negatively charged biomolecules also attaches to polylysine treated surfaces, such as DNA. The cells are normally viable after attachment, though they tend to flatten in an abnormal manner.[67][68] It is demonstrated that PLL absorb the strongest onto a surface at pH levels around 11, this applies to both polar and hydrophilic substrates. Thanks to PLL being, hydrophilic, bio- compatible and -degradable it is valuable for not only cell- and biomolecule adhesion, but also for gene, drug and protein delivery and for bettering attachment of other less adhesive polymers.[69]

The adsorption of PLL onto a surface takes place in a two-step process. In the first step the PLL diffuses from the bulk solution and attaches to the surface. In the second step the PLL rearranges, something which may include repositioning of H-bonds and intramolecular charges.[69][70][71] The rate and amount PLL adsorption is pH-, ionic strength- and temperature dependent.[72]

PLL is known for its antimicrobial activities. It is suggested that thinner coats of PLL have less antimicrobial effects than thick coatings based on research on *e.coli*.[73] The adhesive properties of PLL based on the M_w of the polymers have also been investigated. The higher M_w of the polymer, the larger adhesive force. The PLL that adhered most efficiently had a M_w of 350 kDa and was in solutions of concentrations 0.05-0.1%.[74]

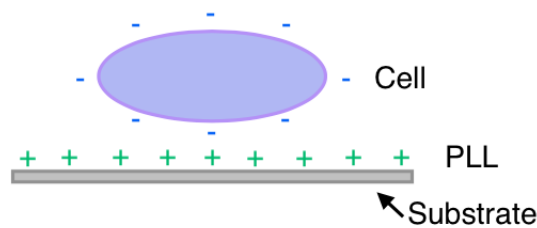

Figure 1.10: A substrate covered with a positively charged PLL-layer, immobilizing a cell with a negatively charged surface.

There are commercially available labeled PLL molecules, such as PLL-FITC. FITC, fluorescein isothiocyanate is a fluorescein derivative. A fluorescent reagent frequently used for biological research purposes due to being easily absorbed and very soluble in water. PLL-FITC is possible to detect with fluorescent microscopy. FITC has an excitation maximum of 490 nm and an emission maximum of 525 nm.[75][76]

1.3.3 Yeast

Saccharomyces cerevisiae, is a species of yeast, often referred to as baker's yeast. It is a single-celled ascomycete, typically of larger size than bacterial cells. *S. cerevisiae* has been used as a model eukaryotic organism for numerous studies. It was the very first eukaryote to have its entire genome sequenced. A model organism is an organism used for various research purposes, making it possible to develop and improve techniques. The findings from studying the model organism is expected to be representative for other organisms.[77][78]

1.3.4 Polystyrene beads

Polystyrene beads are uniform microparticles meant for research and use within biological fields. The beads can be funcionalized by attaching certain chemical groups to their surface, such as amino groups, carboxyl goups, or even proteins and antibodies. These types of beads are produced in sizes from 0.05 μm up to 20 μm.[79][80]

1.4 Imaging methods

1.4.1 Bright field microscopy

Bright field microscopy is an extensively used method for imaging and image analysis of cells and other substances. The method is built upon contrast generation from either changes in absorption of light, colour or refractive index. The most straightforward ways of imaging using bright field microscopy have its restrictions regarding data on the cell outline, position of the nucleus and other large vesicles of unstained samples.[81][82] The advantages of this method are that is a relatively simple and cost-efficient method with little need for much preparation. Staining is sometimes necessary due to low pigmentation in the samples. The optics of bright field microscopy allows the colours from the staining to stay intact, but the staining might damage the sample.[83][84]

1.4.2 Phase contrast microscopy

Phase contrast microscopy gives high-contrast images of transparent samples, such as cells in culture, other microorganism, lithographic patterns and much more. Even organelles could be visualized. By using bright field microscopy it is difficult to obtain good images of basically transparent samples as they hardly absorb any light. To gain a higher clarity and contrast when imaging the samples phase contrast microscopy is often a better alternative. The method manages to increase the contrast without lowering the resolution significantly. The technique comes in handy when examining living cells and their dynamic events. The optical mechanism of phase contrast microscopy is to translate small phase variations into their corresponding amplitudes. If the samples imaged are too thick, the images might look distorted.[82]-[85]

1.4.3 Fluorescence microscopy

Fluorescence is the ability some molecules have to absorb light at a specific wavelength succeeded by emission of light of longer a wavelength. Such

molecules have double bonds in conjugated systems. The time between absorption and emission is called the fluorescent lifetime, which generally lasts less than a μs.[82][86] The sample being investigated is the source of light in fluorescent microscopy. When being irradiated with light of a certain wavelength, the sample will emit energy observable as visible light. Often the sample is not naturally fluorescent, but is rather labelled with fluorescent chemicals. A chemical compound with the ability to re-emit light after being excited is called a fluorophore.[87] In many cases genetic modification of cells is performed to make attachment a fluorescent molecule onto a protein of interest possible. This is useful for investigating gene expression.[83]

Stoke's shift is defined as the loss of vibrational energy when electrons relax back to their ground state from their excited state. The energy loss results in the emission spectrum of an excited fluorophore to be of longer wavelengths than the absorbed light. The larger Stoke's shift, the simpler it is to distinguish between the excitation and emission light.[86] Stoke's shift is explained graphically in figure 1.11.

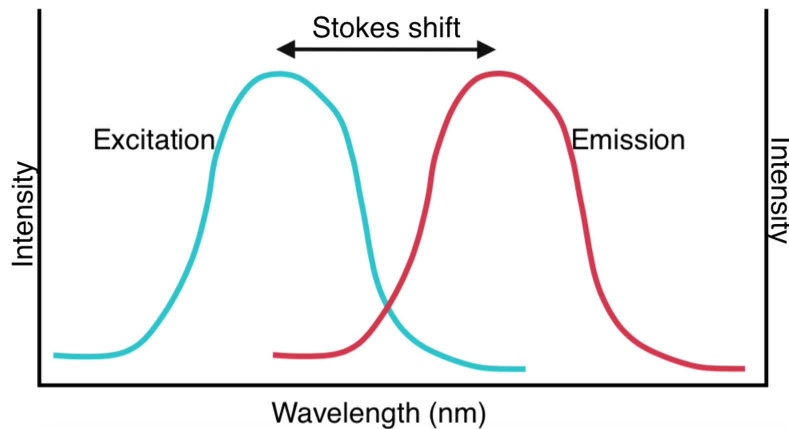

Figure 1.11: The excitation and emission spectra of a fluorophore. The stokes shift is of the spectra is marked on the figure. The emission is of longer wavelengths than the excitation. Adapted from [88].

However, there are some challenges related to fluorescence microscopy. Fluorescence does not last indefinitely. So called photobleaching, fading of the fluorescence, will occur as the samples are being studied. In order to label cells with fluorescence sometimes detergent treatment is necessary to make the cell membranes permeable.[83]

1.4.4 Atomic force microscopy

Atomic force microscopy, AFM, is an imaging technique where the topography of the sample can be found. With AFM surface roughness can be measured with atomic resolution. The technique is utilized in material science and in biological sciences. Both the topography and mechanical properties of cells and extracellular matrices can be investigated using AFM. The AFM set-up has a sharp tip which interacts with the sample surface atoms. Various properties of the surface can be studied by customizing the AFM tip, such as adhesion forces, friction and viscoelasticity.[89][90] A figure of the apparatus set-up of an AFM is given in figure 1.12

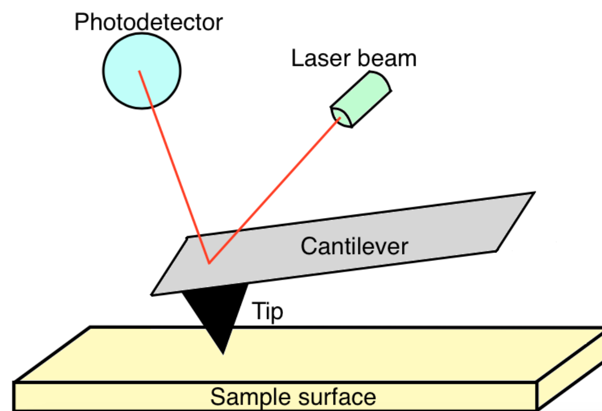

Figure 1.12: Set up of an AFM apparatus. A sharp tip used for scanning of the sample is placed on a flexible cantilever. Usually the radius of the tip is 2-20 nm. Deflection of the cantilever occurs when the tip is in contact with the surface, because of the various forces of the interaction. A laser beam reflects off the back of the cantilever into a photo-detector, measuring the cantilever deflection. There are two different modes of operation when using an AFM, either contact mode or tapping mode. Adapted from [91].

1.5 Aim of the project

The aim of this master thesis is to develop a method for production of microarrays displaying single microorganisms. The arrays are meant to be helpful for exploring the interaction capacities of microorganisms. The main focus was to optimize the process steps in photolithography, PDMS molding and microcontact printing, in order to gain a good procedure that would lead to successful immobilization of microorganisms.
The specific aims were
1. To optimize the photography process; manufacturing a master mold of a quality suited for stamp production. This involved finding the sources of defects and how to correct them, in addition to investigating how different experimental parameters affected the result of the master mold.
2. To investigate the features of PDMS stamps and to which degree PDMS stamps made from various master molds were suited for microcontact printing.
3. To study the effects of different parameters in the microcontact printing process.

2 Materials and methods

2.1 Stamp production

2.1.1 Master mold

The master molds for stamp fabrication were produced using photolithography. 4" silicon wafers were used for this purpose. Master molds on 2" silicon wafers were also prepared. The silicon wafers were cleaned by soaking in acetone followed by washing with isopropanol and ethanol before air drying with N_2. After the washing step, the wafers were baked at 180°C for 15 minutes. An extra cleaning step using a plasma cleaner (Diener Electronics) was included for the majority of the wafers. The wafers were then spincoated with the negative photoresist SU8 (MicroChem). Following the spincoating, the wafers were soft baked before exposure to UV-light through a quartz mask designed with the desired pattern, displayed in figure 2.1. Exposure was done by the use of a maskaligner (Süss MicroTec). Finally, the wafers went through the post-exposure bake before being developed with mrDev 600 developer (micro resist technology) for 1 min under agitation, rinsed with fresh developer, washed with isopropanol and blow dried with N_2.

The times and temperatures for the soft bake and the post- exposure bake for the different types of SU8 photoresist spincoated on the silicon wafers are given in table 2.1.

Table 2.1: Times and temperatures for soft bake and post-exposure bake for the SU8-resist used. The wafers were left on the hotplate while the temperature was ramped up from 65 °C to 96 °C for the soft- and post-exposure bake.

SU8- resist	Soft bake		Post exposure bake	
	time [min]	temp [°C]	time [min]	temp [°C]
SU8-2003,5	1	65	1	65
	2	95	2	95
SU8-5	1	65	1	65
	3	95	3	95

The parameters and settings used for the preparation of the different wafers studied in this project are given in table 2.2. This numbering will be used to refer to various wafers.

Table 2.2: Parameters for the preparations of different silicon wafers into master molds.

#	SU8 resist	Size of wafer [inches]	Plasma cleaned	Spincoating speed [rpm]	UV light exposure dose [mJ/cm^2]
1	SU8-2003,5	4	no	500 (5sec) + 1500 (30 sec)	60
2	SU8-2003,5	4	no	500 (5sec) + 1500 (30 sec)	60
3	SU8-2003,5	2	no	500 (5sec) + 1500 (30 sec)	60
4	SU8-5	2	no	500 (12sec) + 6000 (30 sec)	140
5	SU8-5	4	yes	500 (12sec) + 6000 (30 sec)	140
6	SU8-5	4	yes	500 (12sec) + 6000 (30 sec)	140
7	SU8-5	4	yes	500 (12sec) + 6000 (30 sec)	100
8	SU8-5	4	yes	500 (12sec) + 6000 (30 sec)	120
9	SU8-5	4	yes	500 (12sec) + 3000 (30 sec)	120
10	SU8-5	4	yes	500 (12 sec) + 3000 (30sec)	140
11	SU8-5	4	yes	500 (12 sec) + 3000 (30sec)	130
12	SU8-5	4	yes	500 (10 sec) + 5500 (30sec)	140
13*					

The resist SU8-2003.5 used on wafer 1-3 in table 2.2 was prepared by dilution. SU8-2003.5 contains 37% solids. SU8-2100, containing 75% solids, was diluted with cyclopentanone in order to reach the desired concentration of solids. Dilution was not necessary for the SU8-5 resist used for wafers 4-12.

Wafers number 10 and 11 were prepared with a cooling step after the post bake. They were left on the hotplates until the temperature of the hot plate was approximately 40 °C, allowing them to reach room temperature in a more controlled manner. The same was done following the post exposure bake. Wafer number 12 was prepared with a soft bake temperature of 55°C instead of the temperature given in table 2.1. Wafer number 13 was a wafer prepared by Nina Bjørk Arnfinnsdottir (IFY) and its use was previously proven successful. The wafer was made using a positive photoresist. The pattern of the wafer consisted of 13 circles with diameters increasing form 0.8μm up to 4.4μm.[38]

Figure 2.1 presents microscopy images of the two different patterns of the photo-mask used for preparing wafer 1-12 in table 2.2.

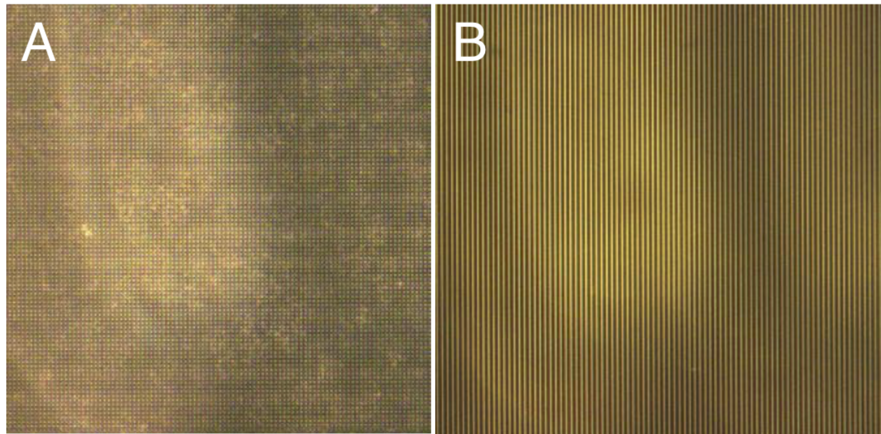

Figure 2.1: The patterns of the photo-mask used during the exposure step in the photolithography process. Part A shows a squared pattern with the dimensions 4 μm, 6 μm and 10 μm. Part B shows a pattern with stripes of widths 10 μm, 8 μm and 5 μm. The spacing between the features were the same size as the feature itself.

2.1.2 PDMS replica molding

A mixture of PDMS curing agent and PDMS base (Sylgard 184, Dow Corning) with a ratio of 1:10 was mixed for approximately 1 minute using a plastic spoon. The mixture was degassed for 5-7 minutes, until sufficient removal of bubbles in the mixture. The desired master mold was put in a container made from aluminum foil before PDMS was poured onto the master mold. Approximately 20 grams of PDMS mixture were used for a 4" wafer and 10 grams for the 2" wafers. The PDMS was then cured for 2 hours at 85°C. After curing the PDMS was peeled gently off the master mold and stored with the pattern side up in a petridish until use.

2.2 Studying PDMS stamps

2.2.1 Imaging of PDMS stamp

Imaging of the features on the prepared PDMS stamps was performed by using phase-contrast microscopy (Zeiss Observer.Z1) with a 20x objective.

2.3 Microcontact printing (μCP)

2.3.1 Printing quantum dots

A 10 nM solution of qdot 655 ITK amino (PEG) quantum dots (Life Technologies) diluted with MQ water was stamped on borosilicate cover glass

slides (VWR international). A piece of the PDMS stamp was cut out using a scalpel and a drop of quantum dot solution covering the array area to be stamped was pipetted onto the stamp before being left to incubate for 10-15 minutes. After incubation excess quantum dot solution was pipetted off and the stamp was blow-dried with N_2. The stamping was performed by placing the stamp pattern side down on the glass slide, applying weight (100 g) and leaving it for 10-15 min.The stamp was carefully removed from the glass slide before the glass slide was studied in a microscope (Zeiss Observer Z.1). Microscopy was done with a 20x objective using the fluorescence filter Cy5 (673 nm).

The PDMS stamps used for printing quantum dots were prepared from wafers 1-3, described in table 2.2. Additionally, a stamp prepared by Nina Bjørk Arnfinsdottir (IFY) was used for this purpose. The stamp was pattern with circular spots with diameters of 3,5 μm with a distance of 10 or 15 μm between each spot.

2.3.2 Printing PLL-FITC and PLL

A 0,5 mg/ml solution of PLL-FITC (Sigma-Aldrich) in MQ-water was prepared and stamped by the same procedure as described in 2.3.1. Both PLL-FITC with molecular weights of 15-30 kDa and 30-70 kDa were stamped. The slides were then investigated by microscopy (Zeiss Observer.Z1)) with a 20x objective using a FITC fluorescence filter.

For stamping of unlabeled PLL a 0,01 % solution (Sigma-Aldrich) with molecular weight 150-300 kDa was used. The procedure was the same as for stamping of PLL-FITC.

2.4 Immobilisation of yeast cells

2.4.1 Yeast cell inoculation

YPD-medium for yeast cell inoculation was prepared by weighing up yeast extract (10 g), bactopepone (20 g), glucose (20 g) and adding MQ-water until the mixture volume was 1 L. The medium was then stirred and autoclaved. Yeast, *Saccharomyces cerevisiae*, was inoculated in 25 ml YPD medium overnight at 180 rpm and 30°C. Autoclaved Erlenmeyer-flasks were used.
1-2 ml yeast cell solution was centrifuged at 4000 rpm for 5 min. The supernatant was discarded and the pellet of cells was dissolved in 1 ml MQ-water before another round of centrifuging at 4000 rpm for 5 minutes. The wash-

ing step was repeated one more time if necessary. The yeast cell solution suited for immobilization was prepared by re-suspending the cell-pellet in 1 ml MOPS buffer (pH 6).

2.4.2 Immobilisation on stamped surface

Yeast cells suspended in MOPS-buffer (1-2 ml) were pipetted onto glass slides stamped with labeled (PLL-FITC) or unlabeled PLL before being incubated for 10 min. After incubation the yeast solution was pipetted off. The slides were gently rinsed off with MQ-water. The slides were studied using phase contrast, bright field and fluorescence microscopy.

2.5 Immobilisation of polystyrene beads

Unlabeled PLL (150-300 kDa) was stamped onto a glass surface as described in sections 2.3.1 and 2.3.2. Stamps prepared from master mold number 13 (described in table 2.2) were used for the printing. The polystyrene beads added to the stamped surface were of diameters 2.10 μm and 3.07 μm functionalized with carboxyl groups (Spherotech). 2 μL of a 5% w/v polystyrene bead solution were thinned up to 200 μL. Polystyrene bead solution were applied to the stamped glass slide, enough to cover the stamped area. The solution were left on the glass slide for 5 minutes before being carefully rinsed off with MOPS buffer. The glass slides were studied using phase contrast and bright field microscopy.

2.6 Investigation of PDMS stamps by AFM

PDMS stamps made from master molds number 7 and 9, their preparation is described in table 2.2, was imaged using an AFM by Gjertrud Maurstad (IFY). Images of parts of the surfaces and topographical data were obtained.

3 Results

3.1 Resist thickness

Table 3.1 shows the measured resist thickness of the different wafers prepared as described in table 2.2. The measurement was performed after the soft bake and before exposure of UV-light. For each wafer ten measurements were performed at various locations on the resist surface.

Table 3.1: Resist thicknesses and their corresponding standard deviations based on ten measurements for each wafer surface. The description of the preparation of the wafers (1-12) is given in table 2.2. For master molds number 5 and 8 all the measurements made on the resist surface is given in appendix A.

Master mold #	Resist thickness [μm]
1	1,94$\pm$0, 49
2	3,80$\pm$0, 12
3	1,37$\pm$0, 03
4	3,13$\pm$0, 18
5	2,91$\pm$0, 13
6	2,85$\pm$0, 01
7	2,83$\pm$0, 005
8	2,88$\pm$0, 13
9	4,82$\pm$0, 04
10	4,86$\pm$0, 09
11	4,79$\pm$0, 18
12	3,03$\pm$0, 007

3.2 Imaging of master molds

The master molds were imaged (Nikon Eclipse LV150) using 20x magnification. Figure 3.1 shows master mold number 2 made with SU8-2003.5 resist. Its preparation is described in table 2.2. Part A of the figure shows a part of the master mold with striped pattern. The stripes are not very apparent. Several bubbles are visible on the stripes parts of the pattern. Part B shows where the pattern in the resist is squared. The squares are of varying visibility. There are also bubbles present on this part of the pattern.

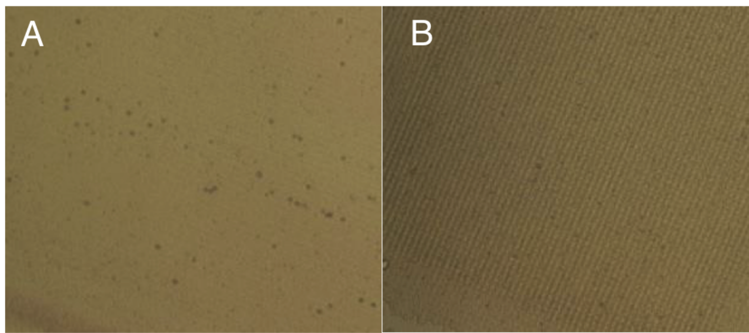

Figure 3.1: Microscopy image with 20x magnification of a wafer covered in SU8-2003.5 resist, wafer number 2 from table 2.2. Part A shows where the resist has a striped pattern, while part B shows where the resist has a pattern consisting of squares. The squares were of dimensions 4 μm, 6 μm, and 10 μm. The stripes were of widths 10 μm, 8 μm and μm.

Figure 3.2 shows images of cracks seen for SU8-5 resists (part A), striped pattern on wafer number 6 (part B) and squared pattern on wafer number 8. Wafers described in table 2.2. In both part B and C cracks are visible.

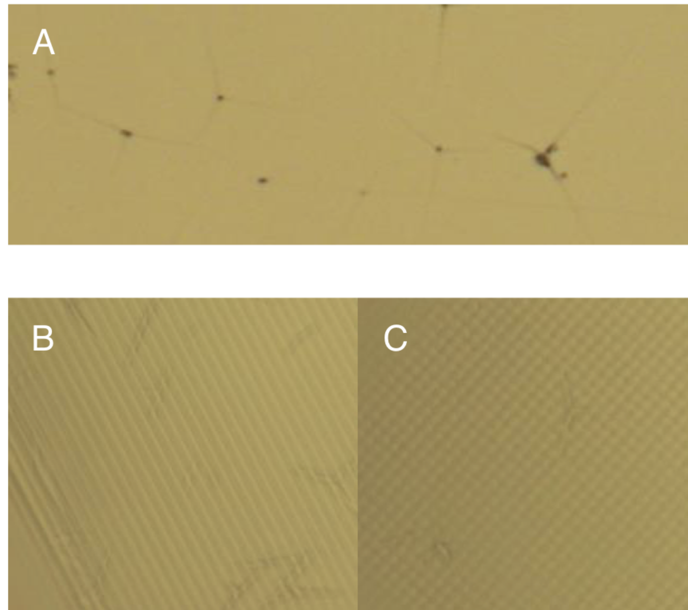

Figure 3.2: Microscopy image with 20 x magnification of SU8-5 covered resist with cracks (A), striped pattern on wafer 6 (B), squared pattern on wafer 8 (C). Wafers described in table 2.2. Wafers 4-12 are prepared using SU8-5 resist.The squares were of dimensions 4 μm, 6 μm, and 10 μm. The stripes were of widths 10 μm, 8 μm and μm.

Figure 3.3 shows both striped and squared pattern on the surface of wafer number 9, wafer prepared as described in table 2.2.

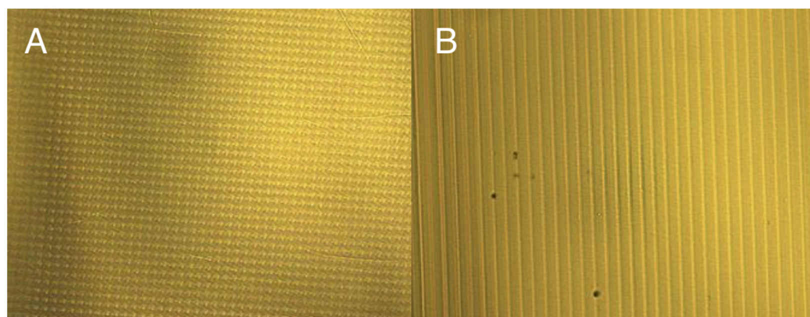

Figure 3.3: Microscopy image with 20x magnification of squared pattern on wafer 9 (B) and its striped pattern (C). Wafers described in table 2.2. The squares were of dimensions 4 μm, 6 μm, and 10 μm. The stripes were of widths 10 μm, 8 μm and μm.

Figure 3.4 shows a wafer covered with a positive type photoresist. The resist layer has a pattern of circles of varying sizes. This master mold is prepared by Nina Bjørk Arnfinnsdottir (IFY).

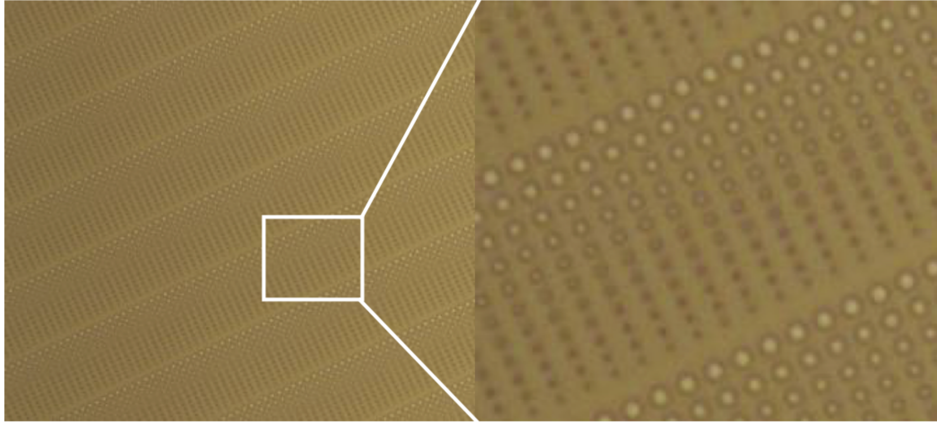

Figure 3.4: Microscopy image with 20x magnification of a master mold patterned with circles of varying sizes, master mold 13 from table 2.2. The circles were of diameters 4.4 μm to 0.8 μm with distances of 7.4 μm, 8.4 μm, 10.4 μm and 12.4 μm.

3.3 Imaging of PDMS stamps

PDMS stamps were imaged using phase contrast. A Zeiss Observer Z1 microscope at 20x magnification was used. PDMS stamps prepared using master molds made with SU8-20003.5 are imaged in figure 3.5. Part A and B displays the squared parts of the pattern. The pattern is more apparent in part A than in part B. The clarity of the pattern also varies between C and D. Some impurities, such as bubbles are seen in A-D.

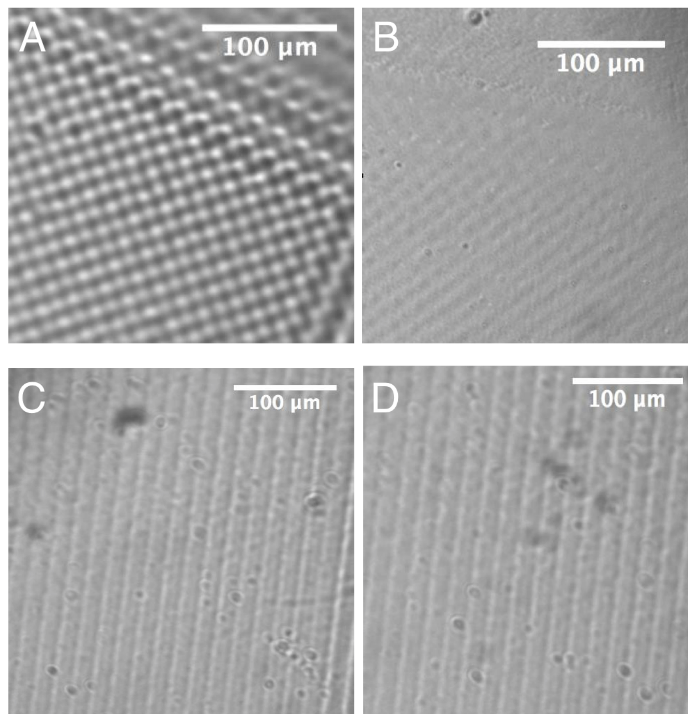

Figure 3.5: Images of PDMS stamps molded on wafer number 3 (described in table 2.2). A and B show the squared pattern. C and D shows the striped pattern.

Figure 3.6 shows various PDMS stamps prepared from master molds made with SU8-5 resist, the stamps are made from master molds 5, 7 and 8. In part A of the figure bubbles and impurities can be seen. In B there are visible cracks. In part C and D the pattern seems to fade, becoming less apparent at certain places. The same type of fading is seen for E and F.

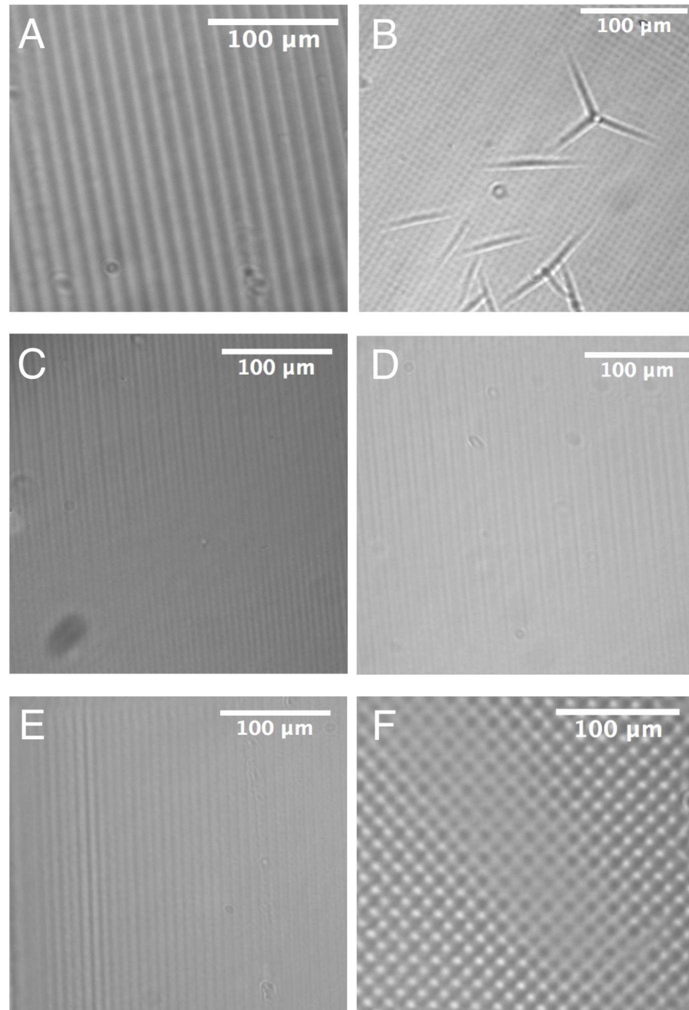

Figure 3.6: Parts A and B of the figure display PDMS stamps with stripe-pattern and square-pattern, respectively. Both are prepared from master mold number 5. C and D both show stripe-patterned PDMS stamps prepared from master mold number 7. E and F shows stripe-patterned and square-patterned PDMS stamps, respectively. Both prepared from master mold number 8.

Figure 3.7 shows PDMS stamps prepared from master mold number 9, 6, 12 and from a master mold prepared by Nina Bjørk Arnfinnsdottir (IFY). The stripe- pattern of the PMDS in part A, prepared from wafer 9, is not very clear, but more apparent than the striped in part C, made from wafer 12, which is hardly seen. The square-pattern in part B, stamp prepared form master mold 9, is visible, but somewhat unclear. Crack-like features can additionally be seen in part B. The stamp prepared from wafer 5, seen in part D, has defined stripe features. E and F display the PDMS stamps prepared from Nina Bjørk Arnfinnsdottir (IFY). The circles are very defined, seen in part E. From part F, a larger overview of the stamp, it is seen that the pattern is very regular and defined over a large part of the stamp.

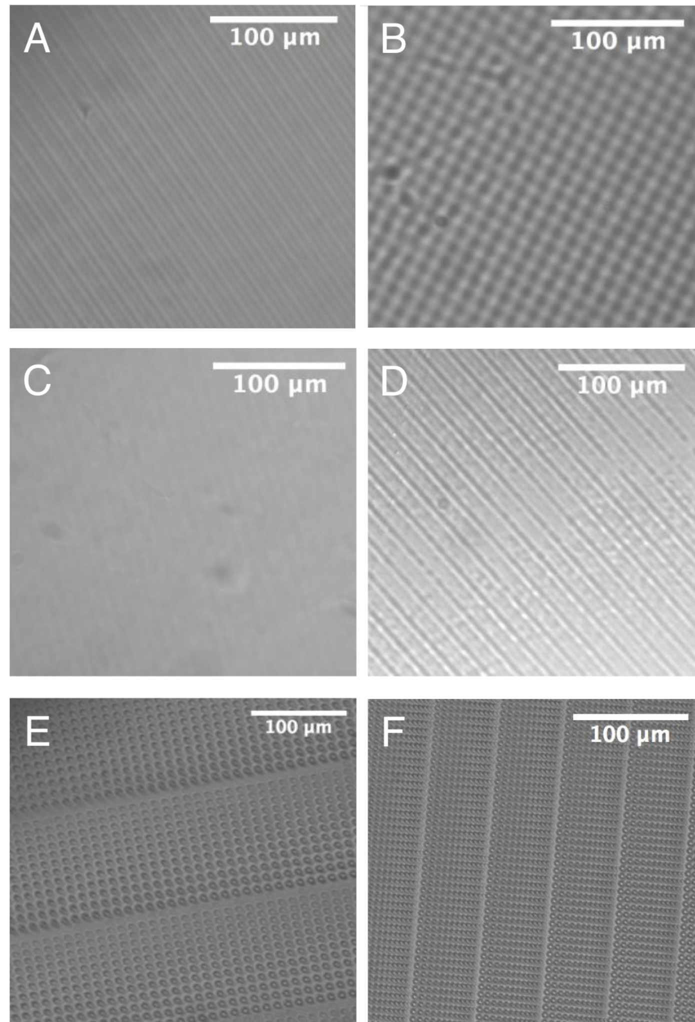

Figure 3.7: Part A and B are PDMS stamps prepared from master mold number 9 and they are stripe-patterned and square-patterned, respectively. Part C is a PDMS stamp prepared from master mold number 12 and stripe-patterned. The PDMS stamp in part D is prepared from master mold number 5, also stripe-patterned. The master molds are prepared as described in table 2.2. E and F are images of PDMS stamps prepared from a master mold made by Nina Bjørk Arnfinnsdottir (IFY). The pattern is circles of varying sizes.

3.4 μCP

3.4.1 Printing quantum dots

Microcontact printed quantum dots were imaged using fluorescence microscopy with the Cy5-filter. A Zeiss Z.1 observer with 20x objective was used.
Figure 3.8 shows microcontact printed quantum dots. The PDMS stamp used for the printing was a stamp prepared by Nina Bjørk Arnfinnsdottir (IFY). The photomask used for its production had a dotted pattern, each dot with a diameter of 3.5 μm with 10 or 15 μm distance between each dot. In part A of the figure the quantum dots are not only in the dotted pattern, but spread over the surface. In part B the quantum dots are printed in the dotted pattern, although they appear somewhat unclear. In part C and D of the image the quantum dots are printed in the dotted pattern but there are additional large spots and aggregations of quantum dots present.

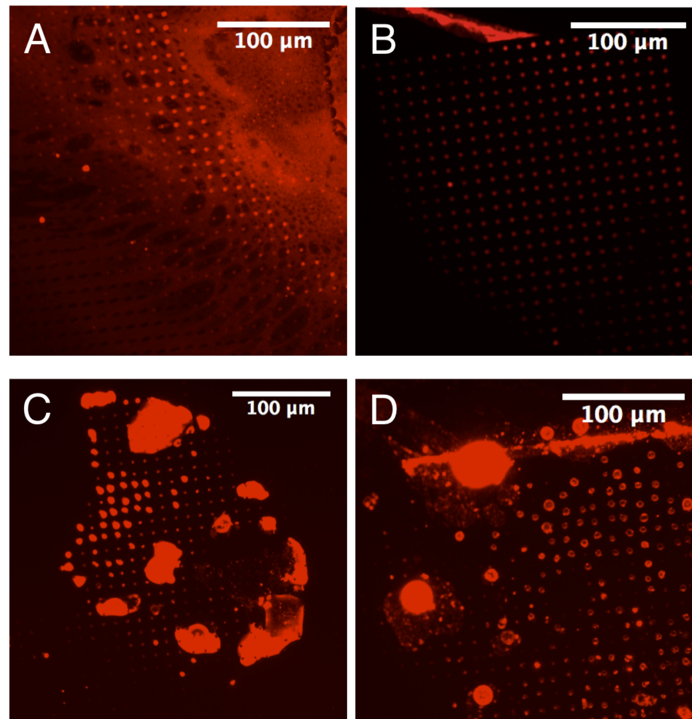

Figure 3.8: μCP QDs imaged with fluorescent microscopy. PDMS stamp used prepared by Nina Bjørk Arnfinnsdottir (IFY). The photomask used for its production had a dotted pattern, each dot with a diameter of 3.5 μm with 10 or 15 μm distance between each dot.

Figure 3.9 shows microcontact printed quantum dots printed with a PDMS stamp prepared from master mold number 3 and 2 (described in table 2.2). In A-D in the figure there is no printed pattern visible. Rather than stripes and squares, irregular spots are visible.

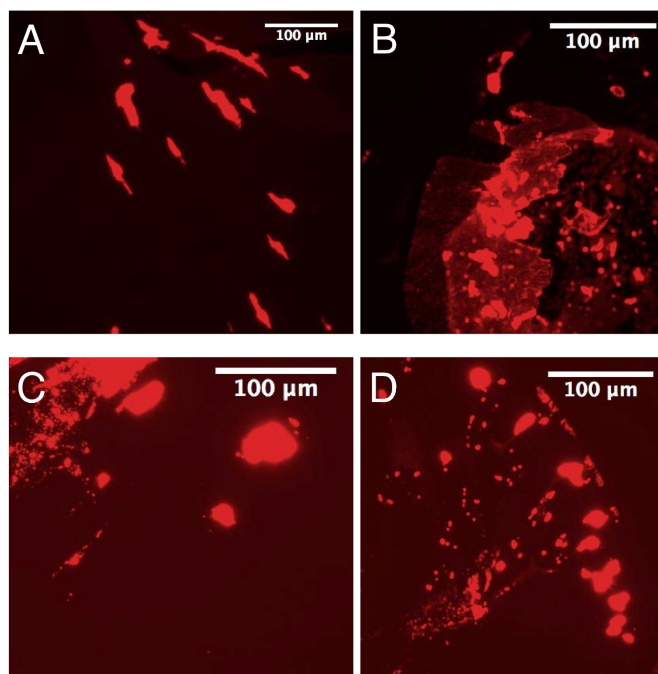

Figure 3.9: μCP of quantum dots. A and B show quantum dots printed using a PDMS stamp prepared from master mold number 2. C and D show quantum dots printed using a PDMS stamp prepared form master mold number 3. Description of master molds are given in table 2.2.

3.4.2 Printing PLL-FITC

μCP of PLL-FITC was imaged using fluorescence microscopy. A Zeiss Z.1 observer with 20x objective was used. Figure 3.10 shows PLL-FITC micro-contact printed using PDMS stamps prepared from master molds 5 and 6 (described in table 2.2, master mold 5 and 6 are prepared using the same parameters). In part A and B of the figure the striped pattern appears quite faint. The pattern is present, although the PLL-FITC is not confined only to the stripes, it appears to be present on most of the imaged surface. The stamped PLL-FITC pattern seems to be clearer in part C, but there are irregularities. In D, E and F the stripes are visible, but only parts of the pattern is successfully transferred onto the surface. Some places the PLL-FITC is not present at all, while other places large, unpatterned spots are seen.

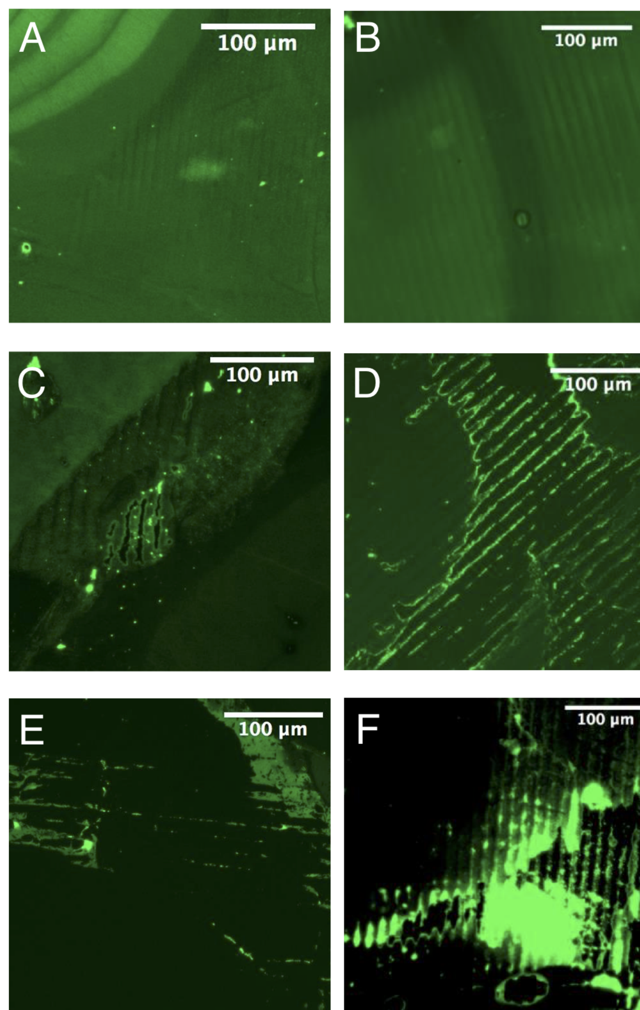

Figure 3.10: μCP of PLL-FITC. The PDMS stamps used for printing are prepared form master molds 5 and 6 (described in table 2.2). A-F in the figure all show printing using the PDMS stamps with striped pattern.

Figure 3.11 shows microcontact printed PLL-FITC. The PDMS stamp used is prepared from master mold number 7 (described in table 2.2). A and B show PLL-FITC attempted pattered in stripes. Only parts of the pattern is printed and there is visible PLL-FITC places other than the pattern. The same can be said for the stamped squared pattern showed in C and D.

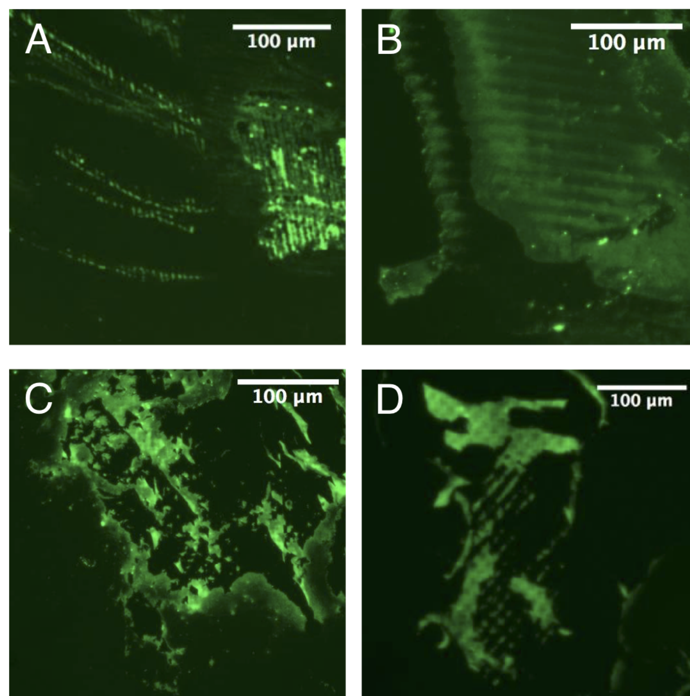

Figure 3.11: μCP of PLL-FITC. The PDMS stamps used for printing are prepared form master mold 7 (described in table 2.2). A and B in the figure show printing using the PDMS stamps with striped pattern, while C and D shows printing using squared pattern.

Figure 3.12 shows PLL-FITC microcontact printed using a PDMS stamp prepared form master mold number 8 (described in table 2.2). Printing of the striped pattern, shown in A-C, is clear at certain areas, but the transfer of PLL-FITC in a striped pattern is only partial. The squared pattern of the stamp can be spotted in D-F. In some areas the PLL-FITC is located around the features rather than on them.

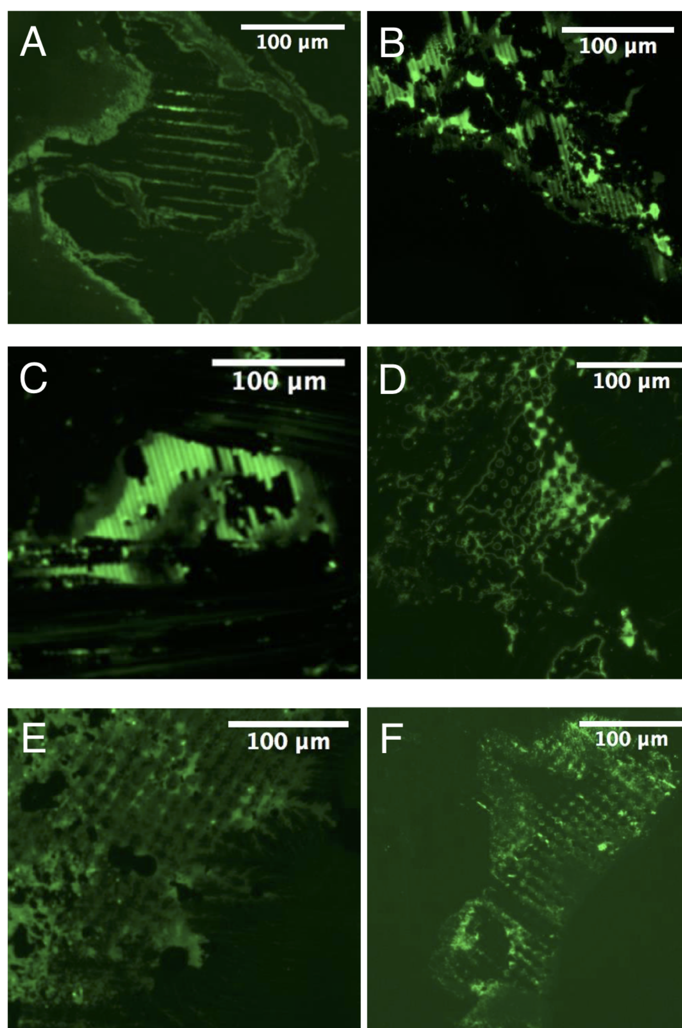

Figure 3.12: μCP of PLL-FITC. The PDMS stamps used for printing are prepared form master mold 8 (described in table 2.2). A-C in the figure show printing using the PDMS stamps with striped pattern, while D-F shows printing using squared pattern

Figure 3.13 shows PLL-FITC microcontact printed using a PDMS stamp prepared form master mold number 9 (described in table 2.2). Part A shows partial striped pattern of PLL-FITC and PLL-FITC on other spots than the pattern. The same can be observed for the squared pattern in C. The PLL-FITC is more evenly distributed in B and D, but it is not only confined to the pattern.

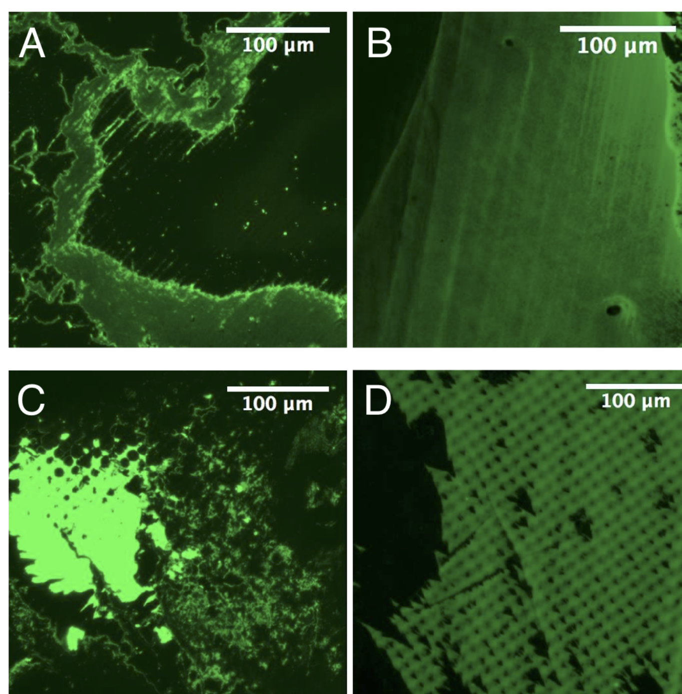

Figure 3.13: μCP of PLL-FITC. The PDMS stamps used for printing are prepared form master mold 9 (described in table 2.2). A and B in the figure show printing using the PDMS stamps with striped pattern, while C and D shows printing using squared pattern. The parts of the stamps used for μCP in B and D were plasma cleaned before stamping.

Figure 3.14 shows microcontact printed PLL-FITC. The stamp used for printing was prepared from master mold number 13 (described in table 2.2). in A, the surface stamped with a non-plasma cleaned stamp, the pattern is visible, but not very clear. In B, the surface stamped with a plasma cleaned stamp the pattern is much clearer than for A.

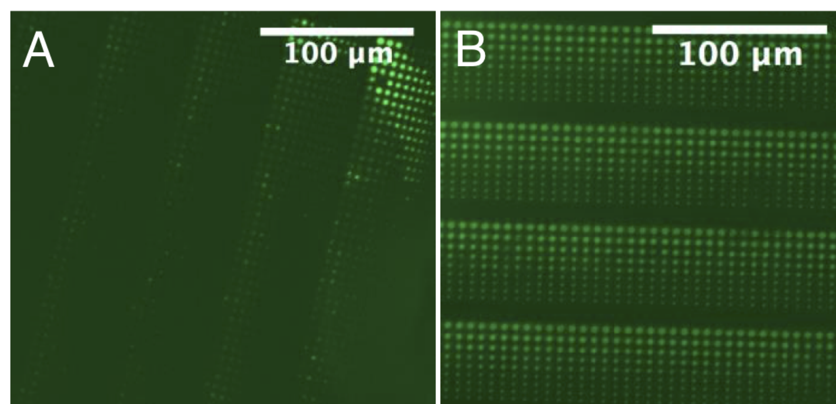

Figure 3.14: μCP of PLL-FITC. The PDMS stamps used for printing are prepared form master mold 13 (described in table 2.2). A and B is PLL-FITC microcontact printed using the same stamp, in B the stamp piece used was plasma cleaned before printing.

3.4.3 Immobilization on functionalized surfaces

Figure 3.15 shows control samples of yeast cells on a glass surface without PLL and on a glass surface with unpatterned PLL. In part A, on the glass slide with no PLL, there are no visible yeast cells. In Part B-C, glass slides with PLL, there are visible yeast cells, often in aggregates.

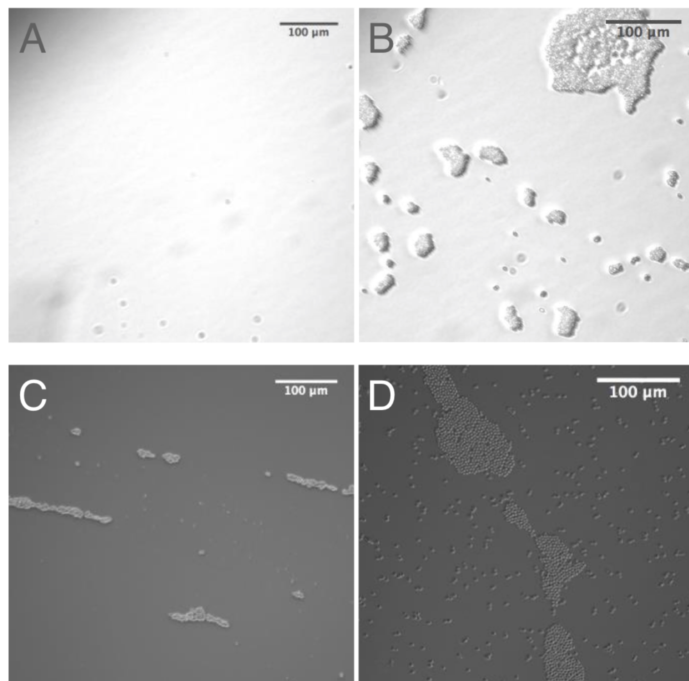

Figure 3.15: A and B are images taken using bright field microscopy with 20x magnification. A shows a clean surface where yeast cells have been attempted mobilized. B shows a glass surface with unpatterned PLL where yeast cells have been attempted immobilized. C and D are images taken using phase contrast microscopy with 20x magnification. Both shows yeast cells attempted mobilized on glass slides with unpatterned PLL.

Figure 3.16 shows yeast cells on a glass slide microcontact printed with PLL-FITC. In part A only the yeast cells are seen. In part B both the yeast cells and the areas where PLL-FITC is located is visible. The areas of stamped PLL-FITC and the location of the yeast cells did not overlap.

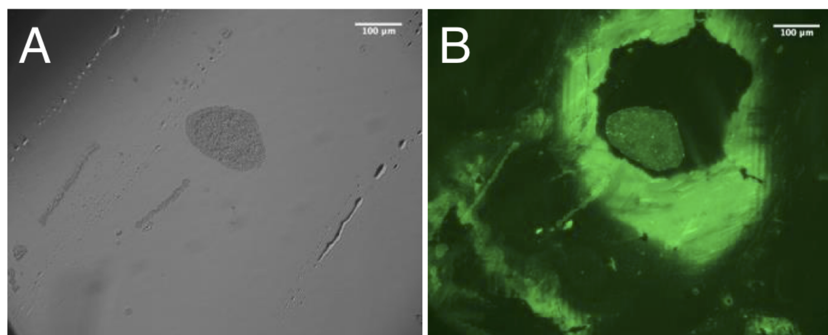

Figure 3.16: Yeast cells on glass slide microcontact printed with PLL-FITC. PDMS stamp used prepared from wafer 8 (described in 2.2 and was stripe-patterned). A is taken using bright filed microscopy and B is taken using fluorescence microscopy.

Figure 3.17 shows yeast cells on surfaces microcontact printed with PLL. For A and B some scattered yeast cells were observed. In C and D the yeast cells were seen in stripe shaped aggregates, in D a larger aggregate was also observed. For E the yeast cells were distributed more evenly, but also here larger aggregates were observed. In A-E, no patterns were observed.

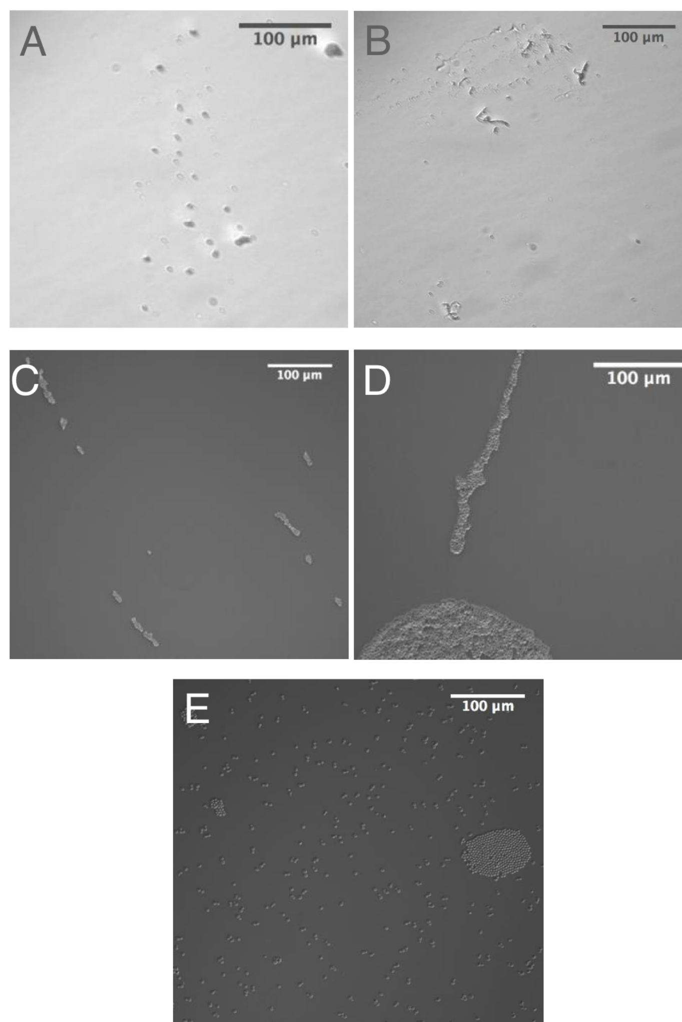

Figure 3.17: Parts A and B was taken using bright field microscopy with 20x magnification. The surface in a was printed using PDMS stamp prepared from master mold number 2, number 3 for B. C- E was taken using phase contrast microscopy with 20x magnification. The surface C was printed using a PDMS stamp prepared from master mold number 3, number 4 for E and number 13 for E.

3.5 Investigation of PDMS stamps by AFM

Measurement of patterned squares

A PDMS stamp prepared from master mold number 8, described in table 2.2, was studies by AFM. The part of the stamp investigated was from the areas patterned with squares. The AFM image obtained is shown in figure 3.18. The image shows regularly repeated features.

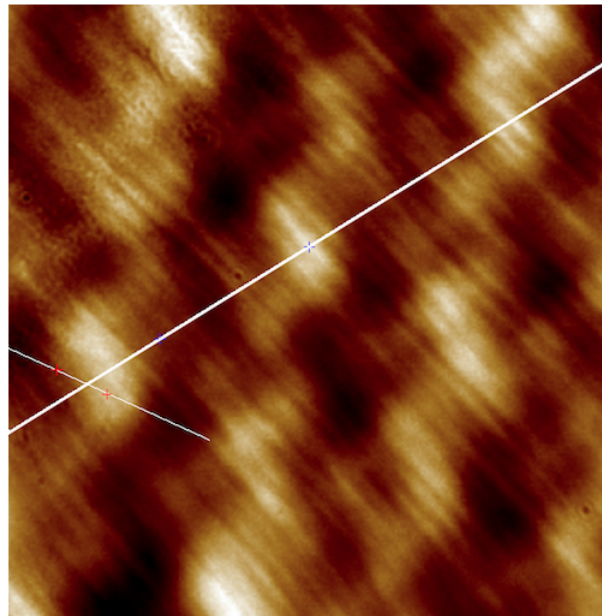

Figure 3.18: An AFM image of a piece of a PDMS stamp with a squared pattern. The stamp is prepared from master mold number 8 given in table 2.2. The white line going across the image shows where the topographical AFM-measurement was done. The light parts of the image represents the highest parts of the stamp features, while the darkest parts represents the lower parts of the stamp features.

Figure 3.19 shows the height of the PDMS pattern plotted against the distance. The height values are given in nm and the length values are given in μm. The The stretch which is measured is shown as a white stripe in figure 3.18. From the plot, three elevations is shown. The height of these elevations are 32.97 nm, 37.57 nm and 33.65 nm. The lowest part of the plot displays the value -17.65 nm, located between the first and the second top. The lowest point between the second and the third top is -12.80 nm.

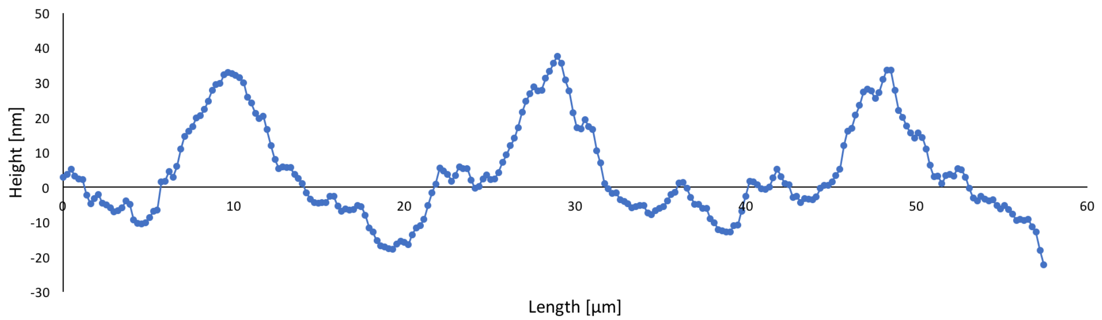

Figure 3.19: Topographical measurement of pattered PDMS by AFM. The x-axis gives the length of the measured area on the PDMS stamp, whereas the y-axis gives the height of the features.

An image of a different part of the same PDMS stamp, prepared from wafer 8 in table 2.2, is given in figure 3.20. The part imaged is patterned with squares.

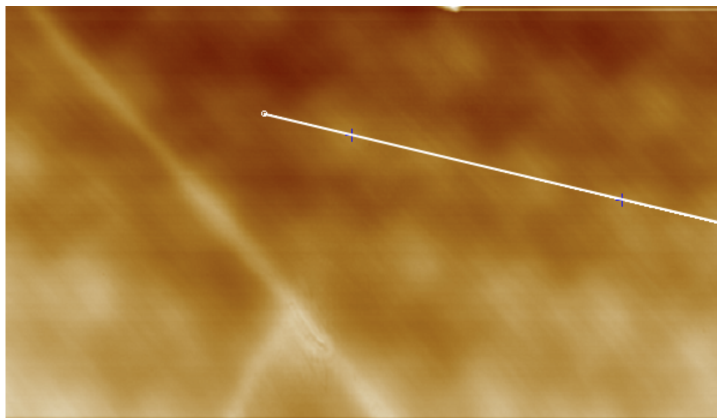

Figure 3.20: AFM image of PDMS stamp prepared from master mold number 8, described in table 2.2. The white line indicates where the topographical measurements were performed.The lighter colour of image, the more elevated is the pattern.

Figure 3.21 shows the height of the PDMS pattern plotted against the distance. The height values are given in nm and the length values are given in μm. The The stretch which is measured is shown as a white stripe in figure 3.20. The plotted graph displays four tops. These tops have height values of 78.34 nm, 72.27 nm, 72,36 nm and 85.20 nm. The valleys between the tops are 35.16 nm, 32.87 nm and 26.31 nm.

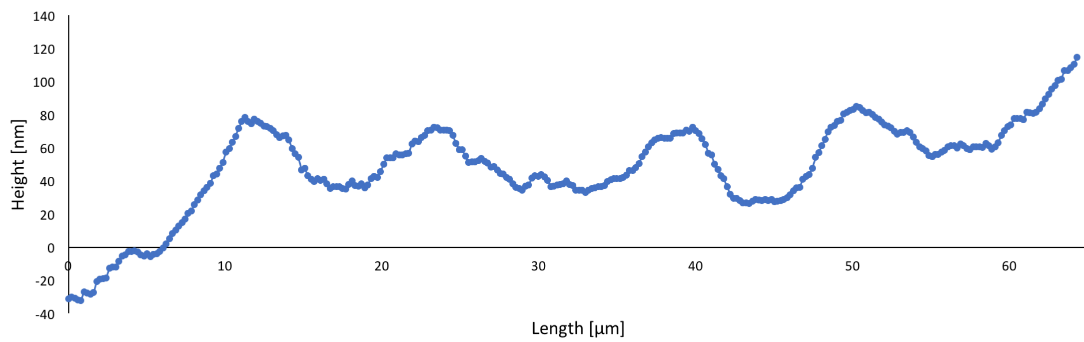

Figure 3.21: Topographical measurement of pattered PDMS by AFM. The x-axis gives the length of the measured area on the PDMS stamp, whereas the y-axis gives the height of the features.

Based on the data achieved from AFM, the width of the features was estimated. An average width from each of the plots was found by measuring the width of every single top. How the widths was measured is illustrated in 3.22. The average width of the four tops in part A of the figure was 5.41 ± 0.17 μm, while for part B the measured average width of the three tops was 6.36 ± 0.57 μm.

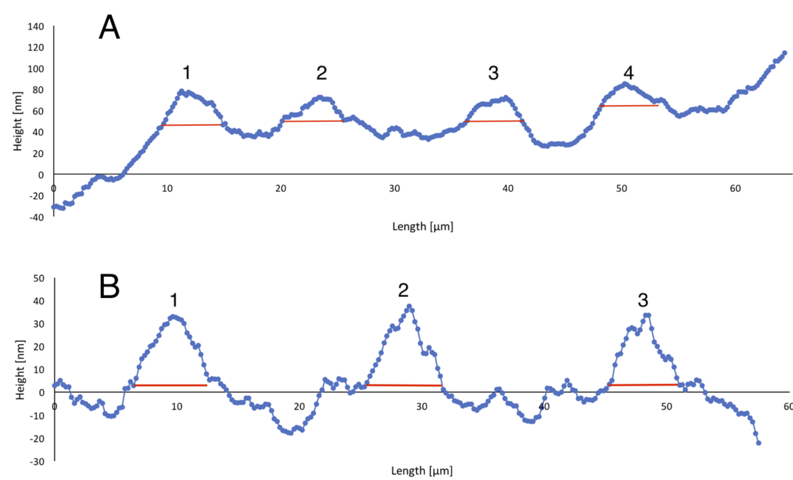

Figure 3.22: The topographical measurement of pattered PDMS by AFM. The red lines mark where the width of each top were measured. Part A of the figure corresponds to the image in figure 3.21 and part B corresponds to 3.18.

Measurement of irregularities

AFM imaging was done of a piece of PDMS stamp prepared using master mold number 9, described in table 2.2. The imaging was performed on parts of the stamp where features other than the desired patterns were observed. Figure 3.23 shows an AFM image of such features. The lines A and B on the figure marks where the topographical measurements were made.

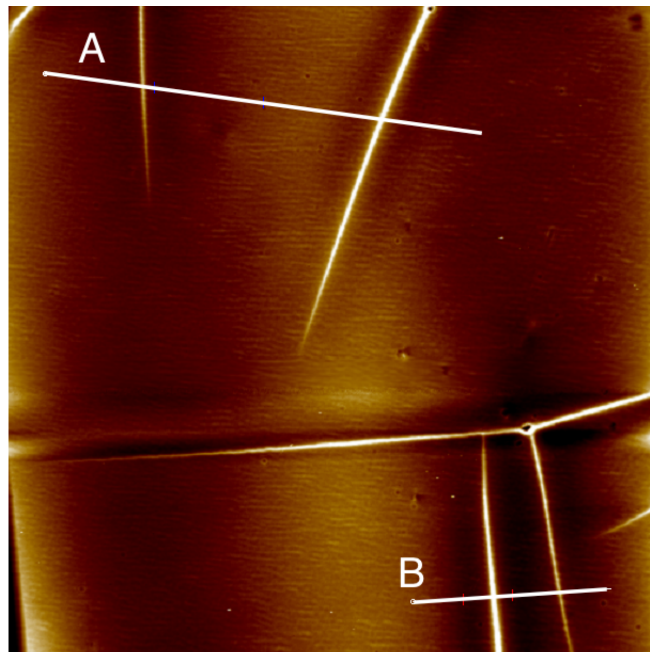

Figure 3.23: AFM image of PDMS stamp prepared from wafer number 9, described in table 2.2. The white lines indicate where topographical measurements were made. The lighter the colour of the image, the more elevated is the features of the PDMS stamp.

The plots of the lines A and B from figure 3.23 is shown in figure 3.24. Both plots have two evident peaks. The peaks in plot A are 26.62 nm and 58.69 nm. The peaks in plot B are 56.14 nm and 28.43 nm. Additionally, the with of the peaks were estimated. The width of the peaks were measured at their widest. For the peaks in plot A the widths were measured to be 4.36 μm and 6,37 μm. For the peaks in plot B the widths were measured to be 4.32 μm and 2,33 μm.

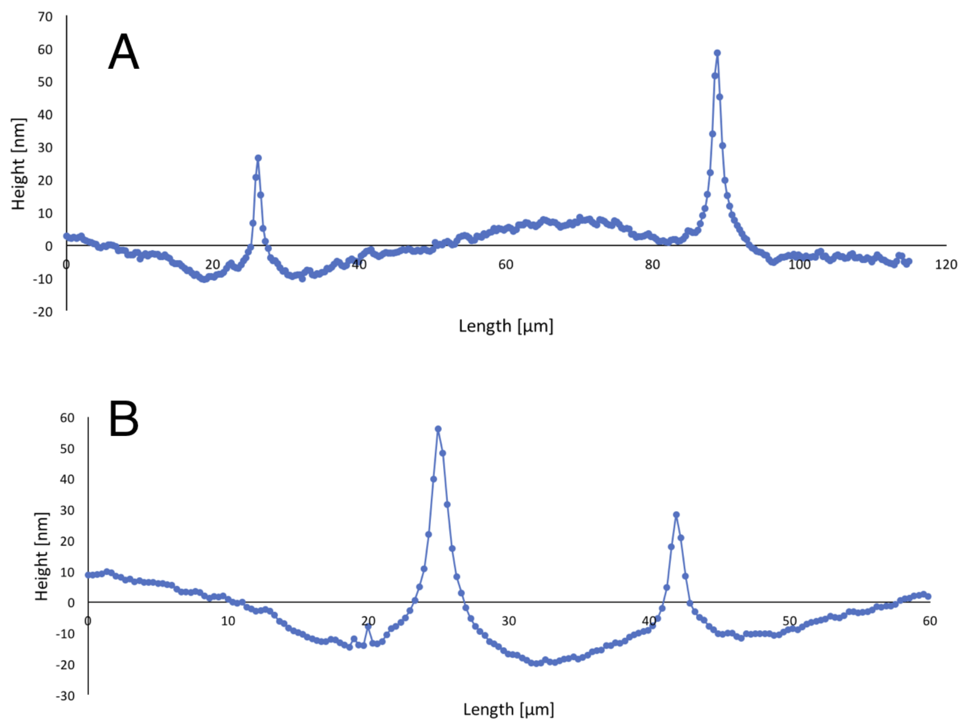

Figure 3.24: Topographical measurement of pattered PDMS by AFM. The x-axis gives the length of the measured area on the PDMS stamp, whereas the y-axis gives the height of the features. The plots A and B corresponds to the lines A and B in figure 3.23.

Another part of the PDMS stamp prepared from wafer number 9 (table 2.2) was investigated. The AFM image is given in figure 3.25.

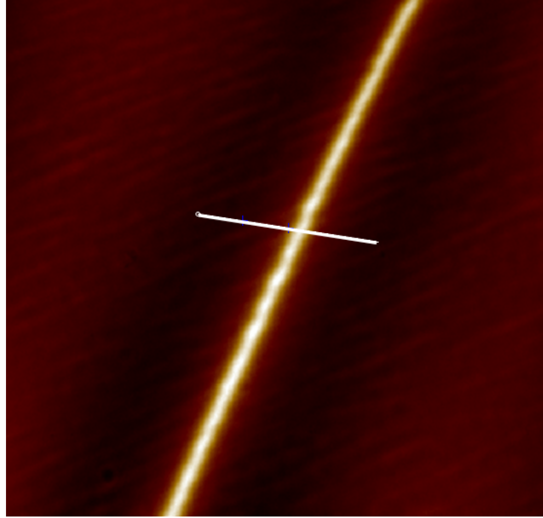

Figure 3.25: AFM image of PDMS stamp prepared from wafer number 9, described in table 2.2. The white line indicates where topographical measurements were made. The lighter the colour of the image, the more elevated is the features of the PDMS stamp

The plot of the line from figure 3.25 is shown in figure 3.26. The plot has one evident peak, with a maximum of 74.52 nm. The with of the peak was estimated. The measurement were done at the widest point of the peak. The width was measured to be 4.25 μm.

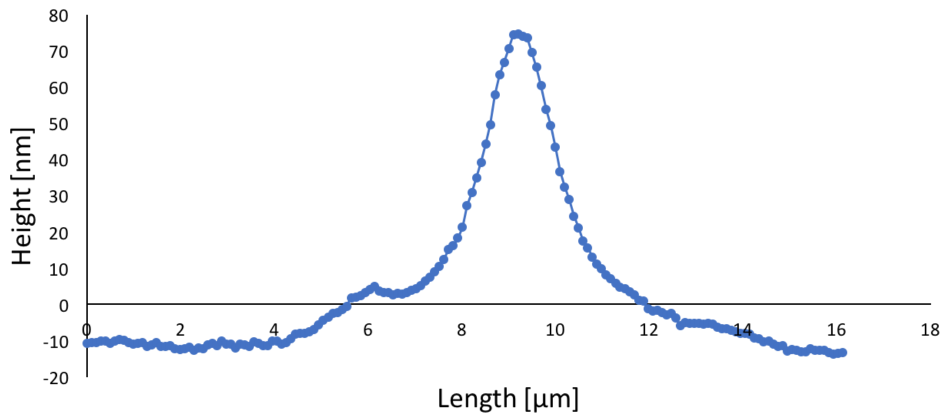

Figure 3.26: Topographical measurement of pattered PDMS by AFM. The x-axis gives the length of the measured area on the PDMS stamp, whereas the y-axis gives the height of the features. The plot corresponds to the line drawn in figure 3.25

4 Discussion

The fabrication of cellular microarrays by the use of photolithograpy, PDMS molding, μCP and immobilization on functionalized surfaces was investigated. Many different experimental parameters and their effects on the process were studied. Errors and flaws of the process were identified and corrections of these errors were researched in order to come closer to optimizing an effective and reproducible process. The effects of each step in the fabrication process on the final result are discussed in the following sections.

4.1 Effect of photolithography parameters

4.1.1 Resist homogeneity

Inhomogeneties in the resist layers on the wafers were observed by several means. Measurement of the layer's thickness at several spots gave an indication of how evenly the resist was distributed on the wafer. Microscopic images of the wafers revealed presence of cracks and bubbles. Often, it was possible to spot defects in the resist layer by eye during the preparation of the wafers. Examples of such defects easily spotted were "comet"-like structures.

Two different types of resist was used and various spin coating speeds were applied. This led to variations in the thickness of the resist layers. The effect of the resist thickness and the homogeneity of the resist layer is important for the quality of the master mold. Inhomogeneity of the resist layer is often considered the main source of complications in lithography processes.[92] Variations in homogeneity can be variations in thickness, irregularities as bubbles or cracks. be The results indicated that the resist layers were not entirely homogeneous. Additionally, edge beads was measured for several of the spin coated wafers. These findings were likely to affect the features of the pattern as an edge bead will cause difficulties during exposure to UV-light. Errors in the pattern of the photoresist will propagate further, causing errors in the features of PDMS stamps and further during μCP.

Resist thickness

As seen from table 3.1 and from table 2.2, the resist thickness was dependant on the spin speed. For the wafers covered in SU8-5 the layers spun with a maximum speed of 6000 rpm was thinner than the layers spun with a maximum speed of 3000 rpm. There was no notable pattern indicating which speed resulted in the most homogeneous layer in terms of thickness. Wafers prepared with the same resist and spin coating speeds, for example wafer

number 5- 8, had some difference in their measured thicknesses. The amount of resist applied before spin coating and the time between application of resist and spinning are parameters likely to have an effect on the resist thickness. SU8-2003.5 and SU8-5 resist had different viscosities, affecting the thickness of the resist layer, making comparison of the spin speeds across resist types difficult.[92]

By comparing the standard deviations of the measured resist thicknesses, it was found that generally the SU8-5 layers were more homogeneous than SU8-2003.5 layers. As a dilution step was necessary for preparation of SU8-2003.5, variations may occur for each batch of this resist. This could be a disadvantage when optimizing experimental parameters.
Thickness measurements was done by measuring ten spots distributed around the surface, which is likely too little data to gain a good overview of the homogeneity of the resist thickness. The resist thickness must be chosen to make the features of the PDMS stamps stable. This is further discussed in section 4.2.

Preparation of both wafers with 2" and 4" diameters were attempted in order to investigate whether there were any difference in resist homogeneity. By using a 2" wafer instead of a 4" wafer the measured resist thickness showed improvement in resist homogeneity for wafers covered with SU8-2003.5, but no improvement was seen for the wafers covered with SU8-5. As there were only one attempt using 2" wafers for each type of resist, it is not possible to say for sure whether or not the wafer size makes a difference for the homogeneity of the resist thickness.

For some of the wafers, based on visual inspection, edge beads were measured. This was observed as a thicker resist layer at the edge of the wafer. Data for the wafers where edge beads were measured is included in appendix A. The measured thickness of the edge beads deviated more from the average thickness of the resist layer than the standard deviation. Insufficient contact between the mask and the resist is likely to take place when an edge bead is present, which may explain why the patterns have some faded areas or why some of them are very unclear.[41][45][46]

Resist irregularities
Irregularities in the resist layer was seen from images of the master molds. The effects of such irregularities were spotted in the images of the PDMS stamps. The spots seen in the resist in figure 3.1 were likely caused by bubble formation in the resist layer, known to occur during dispension of the

resist onto the substrate or because of the N_2 formation due to steady decomposition of the resist's photo active compound.[48] The spots may also have been caused by particles not removed during cleaning. An explanation could be that the wafers shown in figure3.1 were not plasma cleaned before spin coating. As the observed spots appeared to be of the same size or even bigger than the features of the pattern, their impact on μCP were likely very negative.
The cracks seen in figure 3.2 were observed for several of the SU8-5 resist layers, probably arising during or after the soft bake or post exposure bake. Excessive baking and thermal stress could cause cracking with the risk of thermal stress growing bigger with the resist thickness.[42][44][49] Some of the wafers were left on a cooling block after the baking steps, this rapid cool-down could be the cause of cracking. As bubbles, cracks are likely to disrupt the pattern. Wafers with a thicker resist layer, shown in figure 3.3, had a more distinct pattern. A thicker resist layer cause the feature of the pattern to be higher. There were still seen some irregularities for this wafer. In figure 3.4 a wafer with no obvious observable irregularities is pictured, this wafer was made from a positive photoresist.

The quality of the master molds was important for the quality of the PDMS stamps. PDMS stamps molded on wafer number 3, seen in figure 3.5, displayed bubble-like features. This was seen from master molds prepared from the same type of resist, SU8-2005.3. The bubbles in the PDMS stamp could have been caused from insufficient degassing of the PDMS mixture prior to curing.
Figure 3.6 B shows that that the cracked pattern often seen for SU8-5 resist layers was present on the surface of the PDMS stamps. The features of the cracks were much larger and more visible than the features of the stamps. Generally fewer bubbles were seen on these stamps, but fading of the features were seen.
Part A and B from figure 3.7 shows PDMS stamps prepared from wafers with a thicker resist layer. The stripes are perhaps somewhat more prominent than for the the stamps prepared from wafers with thinner resist layers. The same can not be said for the squared pattern. C and D shows PDMS stamps prepared from wafers with relatively similar parameters, only a slight difference in spin speed and thus resist thickness. The one in C being 3.03 μm thick and the one in D 2.91 μm. The pattern in D is much more prominent than the pattern shown in C. This could indicate that even small variations in resist thickness is of importance for the final result. E and F show a PDMS stamp molded from a wafer without any visible impurities. No significant impurities were seen on these stamps. The results argue that even the small-

est impurities from the master molds will have consequences for the quality of the PDMS-stamps.

4.1.2 Exposure doses

Several of the wafers covered with SU8-5 resist were prepared with the same parameters except for the exposure dose in order to find the optimal dose and to investigate the effect of varying it. The PDMS stamps molded from wafers prepared with 100 mJ/cm^2, 120 mJ/cm^2, and 140 mJ/cm^2, shown in figure 3.6, indicated that different exposure doses give features of different qualities. The resist thicknesses of the master molds used were in the range 2.83-2.91 μm. Where 100 mJ/cm^2 was used, the striped pattern was very unclear and faded. For the ones made with higher exposure doses the stripe-pattern was more distinct. A possible explanation for this is underexposure. Underexposure of an SU8-5 resist causes the pattern to dissolve or some of the resist layer to separate from the wafer during developing because of incomplete polymerization.[42][44] The PDMS stamp molded from the wafer where an exposure dose of 140 mJ/cm^2 was used gave the most clear and even striped features, suggesting that this was the most appropriate exposure dose of the ones tested for this resist thickness. However, for the squared features the PDMS stamp molded from the wafer prepared with an exposure dose of 120 mJ/cm^2 was more distinct than for the one where 140 mJ/cm^2 was used. This could have been due to over exposure, caused by formation of acid diffusing to the sides of the exposed areas.[44][42] These findings imply that there were different optimal exposure doses for the two different types of pattern.

4.2 Effect of PDMS stamp quality on μCP

The quality of the PDMS stamps was of importance for how the μCP turned out. Both quantum dots and PLL-FITC was attempted printed onto a glass surface.

μCP of quantum dots
From figure 3.8 the quantum dots printed using PDMS stamps prepared by Nina Bjørk Arnfinnsdottir (IFY) is displayed. These stamps had previously been used for successful μCP.[38] The circular spots of the pattern were clearly visible, but there were several aggregates of quantum dot solution around the pattern. This could indicate that the μCP- procedure was satisfactory, but that the quantum dot solution had aggregated, something

quantum dot solutions tend to do with time.[65] The quantum dots printed using PDMS stamps prepares from master molds covered with SU8-2003.5 resist were not printed in any pattern, only aggregates were seen. These results implies that the batch of quantum dots had aggregated too much to be suitable for printing purposes and that the stamps prepared from the master molds with SU8-2003.5 resist were not suited for printing. Bubbles and impurities were seen from the figures displaying wafers and PDMS stamps made using SU8-2003.5 resist (figures 3.1 and 3.5), possibly explaining why the μCP of quantum dots was unsuccessful. As the quantum dots seemed to aggregate PLL-FITC was used for μCP using the rest of the stamps.

μCP of PLL-FITC

Further μCP was done using PLL-FITC as ink. As PLL is known for its ability to immobilize bacteria onto glass surfaces, this was assumed to be a better way of investigating whether or not the stamps made were suitable for μCP. For the majority of the microcontact printed PLL-FITC only parts of the pattern were transferred onto the glass slide, seen from figures 3.10, 3.11, 3.12 and 3.14. For some of the stamped glass slides the PLL-FITC appeared to be on the edges of the pattern, seen from for example figures 3.10 C and D. This may have been caused by lateral diffusion of of the ink during stamping.[37] No evident connection between which patterns were the most distinct on the PDMS stamps and which stamps gave the best transfer of PLL-FITC onto the glass slides were observed. This suggests that there are factors, not observable by microscopy, which determines how suitable the stamps are for μCP. Plasma cleaning of the PDMS stamps before use gave a more even transfer of PLL-FITC onto the glass slide, even if the PLL-FITC were not clearly transferred in a pattern, seen from figure 3.13. For the PDMS stamp prepared from master mold number 13, a pattern previously proven successful, the effect of plasma cleaning was very evident, seen from figure 3.14.[38] With plasma cleaning the pattern became much more apparent. When plasma cleaning a PDMS stamp, its surface is changed from a hydrophobic to a hydrophilic character. A hydrophobic surface is undesired because it repels polar molecules and cause poor inking of the stamp.[48][54] During the printing procedure it was observed that on untreated stamps the PLL-FITC solution gathered in one large drop on the stamp surface, making it hard to cover the pattern areas. On the plasma treated stamp the solution would spread evenly across the stamp surface. Plasma cleaning had a positive effect on μCP.

For the PDMS stamps prepared from master molds 1-12 the reasons for the inadequate transfer of ink from stamp to surface in the desired patterns

could have been due to various deformations and collapses of the stamp features. Occurrence of deformations depends on the feature's aspect ratios; the height divided by the lateral dimensions. With high aspect ratios buckling and lateral collapse could happen, with low aspect ratios roof collapse could happen.[37][55] The striped features had a width of 10, 8 and 5 μm, assumed that the dimensions of the mask were correctly transferred to the master mold and then to the PDMS stamp. The squared pattern had a width of 4, 6 and 10 μm. The height of the features ranged from 1.94 μm to 4,86 μm. With these dimensions the aspect ratio could not have been high, therefore unlikely that buckling or lateral collapse took place. It is more likely that roof collapse could have happened based on these values. It is however difficult to reach a certain conclusion from the dimensions of the stamps as they could have been, and most likely have been, altered in the process.

AFM results

The results of the AFM measurements indicated that there were repeating features of μm scale present on the surface of the PDMS stamps. The piece of PDMS stamp studied had squared features, which according to the size of the squares on the mask, was expected to be of the sizes 4, 6 or 10 μm. The AFM results stated that the features on the investigated stamp pieces had widths of 5.41$\pm$0.17 μm and 6.36$\pm$0.57 μm. This change of feature size is likely to have happened mainly in the photolithography process, as there are many factors that could cause errors. PDMS shrinks by 1 percent when it is cured, which may also be a part of the explanation to the deviant feature widths.[37][49] From the shape of the plots of the topographical data, seen in figures 3.19 and 3.21, it appears that the features are of different heights and not clearly defined. This would help explain why the μCP was problematic. The distance between the highest and the lowest points measured differed between the two PDMS pieces. The plot from figure 3.19 display a distance varying from 46.45 nm to 55.22 nm. The plot from figure 3.21 displayed distances between maximums and minimums of 115.14 nm and 113.5 nm. The resist thickness of the master mold used for the preparation of this PDMS stamp was 2.88 μm, far from the height of the features according to the AFM measurements. With these dimensions of the stamp features their aspect ratio would be very low, which could cause roof collapses.[37][55]

Cracks formed in the resist layer would cause the PDMS stamp molded from them to have features in the shape of the cracks. The width of the features likely to be caused by resist-cracking in the PDMS stamp measured using AFM ranged from 2.33 μm up to 6.37 μm, being in the same size range as several of the measured and expected features. Crack-features of such sizes

were likely to disrupt the features. The measurements were performed on a PDMS stamp prepared from a master mold with a 4.82 μm thick resist layer. The peaks of the crack shaped features were between 28.43 nm and 74.52 nm in height. This would indicate that when cracks are formed in the resist layer, they do not go through the entire layer.

4.3 Immobilization

When attempting to immobilize yeast cells on both a clean glass slide and a glass slide covered with PLL, a beneficial effect of the PLL was observed. Basically no yeast cells were attached to the clean glass slide, whereas for the slides with PLL many yest cells were seen. The PLL was applied to the slides in one large drop. The cells were expected to attach to the same area where the PLL was applied, but they rather seemed to stay on the glass slide in various aggregates randomly around the surface. An explanation for this could be that the PLL-molecules detached from the glass slide when the yeast cells suspended in buffer were added to the glass slide. Some of the PLL might have been washed away from the glass surface, while some of it stayed in place. The PLL used had a M_w of 150-300 kDa. Studies have found that PLL with M_w of 350 kDa attaches better to glass surfaces than PLL of lower molecular weights.[74] It is possible that PLL of larger molecular weights than used for this experiment would have had better attachment to the surface. However, the results indicate that adding PLL to a glass surface have an effect on yeast cell immobilization. It can also be argued that phase contrast microscopy gives a clearer image of the yeast cells than bright field microscopy as each cell is more visible in the phase contrast images.

Yeast cells were also attempted immobilized on surfaces where PLL-FITC was microcontact printed. In figure 3.16 the same glass slide stamped with PLL-FITC and added yeast cells is imaged using both bright field and fluorescence microscopy. This was done in order to find out where the PLL-FITC was located on the glass slide and whether or not the yeast cells were located in the same place. From the images it is found that the yeast cells did not necessarily attach to every area where PLL-FITC was. The yeast cells seen using bright field microscopy were also seen using fluorescence microscopy, meaning that PLL-FITC attached to the yeast cells. This is explained by the negatively charged cell-surface and the positively charged PLL.[67][68] From the results it is possible to assume that the yeast cells attached to some of the PLL-FITC, but the PLL-FITC does not necessarily stay attached to the glass slide in the wanted pattern. The M_w of the PLL-FITC used ranged from 15-70 kDa, possibly too low for sufficient attachment to the glass slide.

For the yeast cells attempted immobilized on surfaced patterned with unlabeled PLL, shown in figure 3.17, the same kinds of aggregates was seen as for the yeast cells on the glass slides with unpatterned PLL. This would also suggest that the PLL did not stay attached to the surface upon addition of suspended yeast cells, or that the yeast cells did not immobilize on the attached PLL. The image in part E of the figure display more evenly distributed yeast cells than the ones in part A-D. The stamp used for part E was prepared from wafer 13 (described in table 2.2), a stamp with good results for μCP PLL-FITC. The cells were not immobilized in any distinct pattern.

By changing the conditions of the environment, such as pH, ionic strength and temperature, it would be possible to change the rate of PLL adsorption to a surface.[72] Another way of improving the immobilization of yeast cells to patterned PLL could be to treat the glass surface with substrates that prevent bacterial adhesion before patterning the surface. Such substrates are for instance PEG, PVA and BSA. PEG has proven to be especially suitable for this purpose.[38] Alternatively, other chemicals than PLL could be used for immobilizing cells. PEI and PD on glass passivized with PEG have proven to be efficient for cell immobilization.[38]

Yeast cells often have diameters of 4-6 μm.[93] The pattern attempted printed had dimensions of 5, 8 an 10 μm for the stripes and 4, 6 and 10 μm for the squares, giving good reason to assume that if the desired patterns of PLL were properly stamped onto the glass slides and stayed attached, the yeast would be able to be immobilized on the pattern.
Immobilization of polystyrene beads on patterned surfaces were tried without any successful results. The beads had diameters of 2.10 μm and 3.07 μm, smaller than the average yeast cell, but in the size range of some bacterial cells. The beads were functionalized with carboxyl groups, giving reason to think they would attach to the positively charged PLL. An explanation could be detachment of PLL from the glass slides or that the beads simply did not attach to the PLL.

4.4 Quality of results

Relying mainly on images when evaluating the quality of the master molds and the PDMS stamps had some shortcomings. It it difficult to gain information on whether a stamp is suitable for microcontact printing only by looking at an image. Some stamps looked relatively good in the images, but using them for μCP did not provide good results. Here, it was hard to pin down the exact reason for why the stamp was unsuitable for microcontact printing. Additionally, determining which stamps had the most distinct features is likely to be somewhat inaccurate when measured by eye.

The determining of the resist layers would have been more accurate if more than 10 measurements were made around the surface. It would also be possible to say more about the resist layers if more measurements had been performed on the edges, determining if edge beads were present on every wafer and how thick they were.

4.5 Future work

As an optimized photolithography process for producing PDMS stamps suitable for μCP was not found, meaning that further research is needed. Edge beads were measured on the wafers, likely to have caused problems during exposure. The effect of removing of the edge beads would be interesting to investigate.

Further investigation of the PDMS stamps with AFM would give more insight into why μCP did not go well. AFM measurements of stamps molded from master molds prepared with different exposure doses and thickness of resist layers would say more about the effect of each of the parameters in the photolithography process.

5 Conclusion

In this master thesis fabrication of cellular microarrays were investigated. The work aimed to optimize the production process of microarrays and to find the sources of errors in the process. The experimental parameters of the photolithography process were varied in order to optimize the process. SU8-type photoresist were used during photolithography. An inhomogeneous resist layer after spin coating and formations of cracks associated with the baking steps were thought to be large sources of errors, which would cause further problems during UV-light exposure. As there were several challenges related to the use of SU8 photoresist, it should be considered that other types of photoresist may be explored in the place of SU8.

Investigation of PDMS stamps molded from master molds made with SU8 resist using an AFM confirmed that the features of the stamps were not optimal. As did μCP of quantum dots and PLL-FITC. It was seen that plasma cleaning of PDMS stamps before inking was beneficial.

PLL were stamped onto glass slide in order to immobilize cells onto the stamped pattern. As this did not turn out successful there should be considered using either PLL of higher M_w (more than 300 kDa) or using other chemicals. For instance covering the glass surface with PEG, inhibiting cellular attachment and then stamping the surface with PEI or PD, known to immobilize cells.

From thoroughly investigating every step in the fabrication process it was found that the methods used for PDMS molding and μCP were most likely sufficient. The errors in the process originated mainly from the photolithography process and from the chemicals chosen as immobilizing agents.

Bibliography

1. DE SOUZA, N. 2011 Single Cell Methods. Nature Methods, VOL.9 NO.1, January 2012, p. 35.
2. LIDSTRØM M.E. & KONOPKA, M.C. 2010 The role of physiological heterogeneity in microbial population be- havior. Nature chemical biology 6, p. 705–712.
3. GEFEN, O. & BALABEN, N.Q., 2009 The importance of being persistent: heterogeneity of bacterial populations under antibiotic stress. FEMS Microbiol ReV 4, p 704-17.
4. WOOD, T.K. & KNABEL, C. & KWAN, W. 2013 Bacterial Persister Cell Formation and Dormancy. Applied and Environmental Microbiology v.79(23), p 7116-7121.
5. HOBBY, G.L. & MEYER, K. & CHAFFEE, E. 1942 Observations on the mechanism of action of penicillin. Proceedings of the Society for Experimental Biology and Medicine 50, p 281–285.
6. BIGGER, J.W. 1944. Treatment of staphylococcal infections with penicillin by intermittent sterilisation. Lancet 244, p 497–500.
7. LEWIS, K. 2010. Persister cells. Annual Review of Microbiology 64, p 357–372.
8. STEWART, G.R., ROBERTSON, B.D. & YOUNG, B.D. 2003 Tuberculosis: a problem with persistence. Nature Reviews Microbiology 1, p 97–105.
9. Lewis, K. 2001 Riddle of Biofilm Resistance. Antimicrobial Agents and Chemotherapy. 2001;45(4), p 999-1007.
10. LEWIS, K. 2007. Persister cells, dormancy and infectious disease. Nature reviews. Microbiology, 5(1), p 48–56.
11. LEWIS, K. 2001. Antimicrobial agents and chemotherapy, 45(4), p 999–1007.
12. HOCHBAUM, A.I. & AIZENBERG, J 2010. Bacteria pattern spontaneously on periodic nanostructure arrays. Nano letters 10, p 3717–21.
13. MSADEK, T. 1999. When the going gets tough: survival strategies and environmental signaling networks in Bacillus subtilis. Trends in Microbiology, 7(5), p 201–207.
14. VEENING, J.W., SMITS, W.K., & KUIPERS, O.P. 2008. Bistability, epigenetics, and bethedging in bacteria. Annual review of microbiology, 62, p 193–210.
15. DUBNAU, D. & LOSICK, R. 2006. Bistability in bacteria. Molecular Microbiology, 61, p 564–572.
16. KÆRN, M., ELSTON, T.C., BLAKE, W.J. & COLLINS, J.J. 2005. Stochasticity in gene expression: from theories to phenotypes. Nature Reviews Genetics, 6(6), p 451–464.

17. ACKERMANN, M. 2015. A functional perspective on phenotypic heterogeneity in microorganisms. Nature Reviews Microbiology, 13(8), p 497–508.
18. LOCKE, J.C.W. & ELOWITZ, M.B. 2009. Using movies to analyse gene circuit dynamics in single cells. Nat. Rev. Microbiol. 7, p 383–392.
19. BLAKE, W.J., KAERN, M., CANTOR, C.R. & COLLINS, J.J. 2003. Noise in eukaryotic gene expression. Nature 422, p 633–637.
20. ROBERTSON, S. 2014. What is Flow Cytometry. News Medical Life Sciences, http://www.news-medical.net/life-sciences/What-is-Flow-Cytometry.aspx.
21. BIOPROBES® 70. 2014. Image Live Cells Through Time and Space, Optimizing conditions for time-lapse fluorescence microscopy. lifetechnologies.com.
22. WEIBEL, D.B., DILUZIO, W. R. & WHITESIDES, G. M. 2007, Microfabrication meets microbiology. Nature 5, p 209-218.
23. JONCZYK, R., KURTH, T,. LAVRENTIEVA, A., WALTER, J.G., SCHEPER, T. & STAHL, F. 2016. Living Cell Microarrays: An Overview of Concepts. Microarrays 2016, 5(2), 11 doi:10.3390/microarrays5020011
24. MADIGAN, M., MARTINKO, K., BENDER, K., BUCKLEY, D. & STAHL, D. 2015. Brock Biology of Microorganisms, 14th edition, Pearson, p 223.
25. HALL. D.A., PTACKEK, J. & SNYDER, M. 2007. Protein Microarray Technology. Mechanisms of Ageing and Development, 128(1), p 161–167.
26. WATANABE, A., CORNELISON, R. & HOSTETTER, G. 2014. Tissue microarrays: applications in genomic research. Expert Review of Molecular Diagnostics, p 171-181.
27. YARMUSH, M.L. & KING, K.R. 2009. Living-Cell Microarrays, Annual Review of Biomedical Engineering Vol. 11, p 235-257.
28. ELAD, T. & LEE, J.H. 2009. Microbial whole-cell arrays. Microbial Biotechnology, 1(2), p 137–148.
29. VAN DYK, T.K., DEROSE, E.J. & GONYE, G.E. 2001. LuxArray, a high-density, genomewide transcription analysis of Escherichia coli using bioluminescent reporter strains. J Bacteriol. 2001;183, p 5496–5505.
30. MELAMED, S., ELAD, T. & BEKIN, S. 2011. Microbial sensor cell arrays. Current Opinion in Biotechnology (23), p 2-8.
31. KIM J.H., LEE, D.Y., HWANG, J. & JUNG, H.I. 2009, Direct pattern formation of bacterial cells using micro droplets generated by electrohydrodynamic forces. Microfluidics and Nanofluidics 7, p 829–839.
32. MOSSOBA,M.M., AL-KHALDI, S.F., KIRKWOOD, J., FRY F.S., SEDMAN, J. & ISMAIL, A.A.2005 Printing microarrays of bacteria for

identification by infrared microspectroscopy. Vibrational Spectroscopy 38, p 229–235.
33. ROZHOK, S., NYAMJAV, D., LIU, C., MIRKIN, C.A. & HOLZ, R.C. 2006 Attachment of motile bacterial cells to prealigned holed microarrays. Langmuir 22, p 11251–4.
34. FORMOSA, C., PILLET, F., SCHIAVONE, M., DUVAL, R.E., RESSIER, L. & DAGUE, E. 2015. Generation of living cell arrays for atomic force microscopy studies. Nature Protocols. 10, 199–204 doi:10.1038/nprot.2015.004
35. RUIZ, S.A & CHEN, C.S. 2007. Microcontact printing: A tool to pattern. Soft Matter (3), p 168-177.
36. WILBUR, A., KUMAR, A., BIEBUYCK, H.A., KIM, E. & WHITESIDES, G.M. 1996. Microcontact printing of self-assembled monolayers: applications in microfabrication. Journal Nanotechnology 7, 4, 452.
37. PERL, A., REINHOUDT, D.N. & HUSKENS, J. 2009. Microcontact Printing: Limitations and Achievements. Advanced Materials 21(22), p 2257 - 2268.
38. ARNFINNSDOTTIR, N.B., OTTESEN, V., LALE, R., SLETMOEN, M. 2015. The design of simple bacterial microarrays; Development towards immobilizing single living bacteria on predefined micro-sized spots on patterned surfaces. Plos one 10 (6).
39. HONG, X. 2012. Introduction to Semiconductor Manufacturing Technology. Society of Photo Optical. 2nd edition. p 179.
40. MICROCHEM. 2017. Lithography terms.
http://www.microchem.com/Tech-LithoTerms.htm.
41. HONG, X. 2012. Introduction to Semiconductor Manufacturing Technology. Society of Photo Optical. 2nd edition. p 181-182, 192
42. MICROCHEM. Negative Tone Photoresist Formulations 50-100
http://www.microchem.com/pdf/SU8_50-100.pdf
43. LIU, J., CAI, B. & ZHU, J. et al. Microsystem Technologies (2004) 10: 265. doi:10.1007/s00542-002-0242-2
44. MARTINEZ-DUARTE, R. & MADOU, M.J. 2010. SU-8 Photolithography and Its Impact on Microfluidics, Microfluidics and Nanofluidics Handbook: Fabrication, Implementation and Applications, Edition: 1, Chapter: 8, Publisher: CRC Press, p. 231-268
45. LUDWIG, M., FRADEN, S. & BANDOO, K. 2015. A simple and inexpensive device to remove edge beads. Royal society of chemistry. Chips and Tips. http://blogs.rsc.org/chipsandtips/2015/03/02/a-simple-and-inexpensive-device-to-remove-edge-beads/?doing_wp_cron=1495208747.5773530006408691406250.
46. PRAKASH, S. & YEOM, J. 2014. Nanofluidics and Microfluidics: Systems and Applications.

47. MICROCHEMICALS. 2013. Lithography trouble shooter.
http://www.microchemicals.com/technical_information
/TroubleShooter_EN.pdf. retrieved 05.06.17
48. KAUFMANN, T. & RAVOO, J. 2010. Stamps, inks and substrates: polymers in microcontact printing. Polymer Chemistry 1.4 p 371.
49. ZHANG, J., TAN, K.L., HONG, G.D., YANG, L.J. & GONG, H.Q. 2001. Polymerization optimization of SU-8 photoresist and its applications in microfluidic systems and MEMS. J Micromech Microeng. 11 p 20–6.
50. LÖTTERS, J.C., OLTHUIS, W., VELTNIK, P.H. & BERGVELD, P. 1997. The mechanical properties of the rubber elastic polymer polydimethylsiloxane for sensor applications. Journal of Micromechanics and Microengineering, 7 p 145–147.
51. DOW CORNING. 2014. Sylgard 184 Silicone Elastomer Kit.
52. GRAHAM, D.J., PRICE, D.D. & RATNER, B.D. 2002. Solution Assembled and Microcontact Printed Monolayers of Dodecanethiol on Gold: A Multivariate Exploration of Chemistry and Contamination. Langmuir 18.5 p. 1518–1527.
53. PETRZELKA, J.E. & HARDT, D.E. 2012. Static load-displacement behavior of PDMS microfeatures for soft lithography. Journal of Micromechanics and Microengineering 22.7
54. TAN, S.H., NGUYEN, N.T., CHUA, Y. C. & KANG, T.G. 2010. Oxygen plasma treatment for reducing hydrophobicity of a sealed polydimethylsiloxane microchannel. Biomicrofluidics, 4(3).
55. SHARP, K.G., BLACKMAN, G.S., GLASSMAKER, N.J., JAGOTA, A. & HUI, C.Y. 2004. Effect of stamp deformation on the quality of microcontact printing: theory and experiment. Langmuir.20(15):6430-8.
56. XIA, Y. & WHITESIDES, G.M. 1998. Soft Lithography. Annual Review of Materials Research (28) p. 153–84.
57. KUMAR, A. & WHITESIDES, G.M. 1993. Features of gold having micrometer to centimeter dimensions can be formed through a combination of stamping with an elastomeric stamp and an alkanethiol “ink” followed by chemical etching. Applied Physics Letters 63, 2002.
58. BERNARD, A., DELAMARCHE, E., SCHMID, H., MICHEL, B., BOSSHARD, H.R. & BIEBUYCK, H. 1998. Printing Patterns of Proteins. Langmuir, 14 (9), p 2225–2229.
59. ANDERSON, A.B. & ROBERTSON, C.R. 1995. Absorption spectra indicate conformational alteration of myoglobin adsorbed on polydimethylsiloxane. Biophysical Journal, 68(5), p 2091–2097.
60. SABELLA, S., BRUNETTI, V, TORRE, A.D., RINALDI, R. CINGOLANI, R. & POMPA, P. 2009. Micro/Nanoscale Parallel Patterning of

Functional Biomolecules, Organic Fluorophores and Colloidal Nanocrystals. Nanoscale Research Letters, 4(10), p 1222–1229.
61. LANGE, S., BENES, V., DIETER, P., HÖRBER, H., & BERNARD, A. 2004. Microcontact Printing of DNA Molecules. Analytical Chemistry 76 (6), p 1641–1647.
62. THIBAULT, C., BERRET, V.L, CASIMIRIUS, S., TREVISIOL, E., FRANCOIS, C. & VIEU. C. 2005. Direct microcontact printing of oligonucleotides for biochip applications. Journal of Nanobiotechnology 3:7.
63. SIGMA-ALDRICH. 2017. Quantum dots.
http://www.sigmaaldrich.com/technical-documents/articles/
materials-science/nanomaterials/quantum-dots.html.
64. EKIMOV, A & ONUSCHENKO, A.A. 1981. Quantum size effect in three-dimensional microscopic semiconductor crystals. JETP Letters, 43 (6), p 345.
65. THERMO FISHER SCIENTIFIC. 2017. Qdot™ 655 ITK™ Carboxyl Quantum Dots.
https://www.thermofisher.com/order/catalog/product/Q21321MP.
66. SIGMA ALDRICH. 2017. Poly-L-lysine hydrobromide.
http://www.sigmaaldrich.com/catalog/product/sigma/p2636?lang
=enregion=NOcm_sp=Insite-_-prodRecCold_xviews-_-prodRecCold10-3.
67. MAZIA, D., SCHATTEN, G. & SALE, W. 1975. Adhesion of cells to surfaces coated with polylysine. Applications to electron microscopy. The Journal of Cell Biology. 66 (1): 198.
68. GUO, A. 2015. Polylysine surfaces. Microsurfaces, Inc.
http://www.proteinslides.com/polylysine.
69. CHOI, J.H., KIM, S.O., LINARDY, E. DREADEN, E.C., ZHDANOV, V.P., HAMMOND, P.T. & CHO, N.J. 2015. Influence of pH and Surface Chemistry on Poly(l-lysine) Adsorption onto Solid Supports Investigated by Quartz Crystal Microbalance with Dissipation Monitoring. The Journal of Physical Chemistry B. 119 (33), p 10554–10565.
70. HARTVIG, R.A., VAN DE WEERT, M., ØSTERGAARD, J., JORGENSEN, L. & JENSEN. 2011 H.Protein adsorption at charged surfaces: The role of electrostatic interactions and interfacial charge regulation. Langmuir. 27 (6) p 2634– 2643.
71. RABE, M., VERDES, D. & SEEGER, S. 2011. Understanding protein adsorption phenomena at solid surfaces. Advances in Colloid and Interface Science. 162 (1–2) p 87– 106.
72. PORUS, M. MARONI, P. & BORKOVEC, M. 2012. Response of adsorbed polyelectrolyte monolayers to changes in solution composition. Langmuir 28 (50) p 17506– 17516.
73. COLVILLE, K., TOMPKINS, N. RUTENBERG, A.D. & JERICHO,

M.H. 2010. Effects of poly(L-lysine) substrates on attached Escherichia coli bacteria. Langmuir. 16;26(4) p 2639-44.
74. HUANG, W.M., GIBSON, S.J., FACER, P., GU, J. & POLAK, J.M. 1983. Improved section adhesion for immunocytochemistry using high molecular weight polymers of L-lysine as a slide coating. Histochemistry. 77(2) p 275-9.
75. THERMO FISHER SCIENTIFIC. 2017. Fluorescein (FITC).
https://www.thermofisher.com/no/en/home/life-science/cell-analysis/fluorophores/fluorescein.html.
76. SIGMA ALDRICH. 2017. Poly-L-lysine–FITC Labeled.
http://www.sigmaaldrich.com/catalog/product/sigma/p3543.
77. MADIGAN, M., MARTINKO, K., BENDER, K., BUCKLEY, D. & STAHL, D. 2015. Brock Biology of Microorganisms, 14th edition, Pearson, p 584.
78. KARATHIA, H., VILAPRINYI, E. SORRIBAS, A. & ALVES, R. 2011. Saccharomyces cerevisiae as a model organism: a comparative study. PLoS One. 2;6(2).
79. SPHEROTECH. 2017. About Spherotech.
http://www.spherotech.com/about.htm.
80. SPHEROTECH. 2017. Functionalized Polystyrene Particles - Carboxyl.
http://www.spherotech.com/carboxyl.htm.
81. REYES-ALDASORO, C.C. 2015. Bright Field Microscopy, in Biomedical Image Analysis Recipes in MATLAB®: For Life Scientists and Engineers, John Wiley Sons, Ltd, Chichester, UK.
82. ROTTENFUSSER, R., WILSON, E.E. & DAVIDSON, M.V. 2016. Education in Microscopy and Digital Imaging. Zeiss.
http://zeiss-campus.magnet.fsu.edu/articles/basics/contrast.htmlbrightfield
83. WILSON, S.M. & BACIC, A. 2012. Preparation of plant cells for transmission electron microscopy to optimize immunogold labeling of carbohydrate and protein epitopes. Nature Protocols 7, p 1716–1727.
84. KIM, O. 2016. Phase Contrast vs. Bright Field Microscopy.
http://www.microbehunter.com/phase-contrast-vs-bright-field-microscopy/.
85. MURPHY, D.B., OLDFIELD, R., SCHWARTZ, S. & DAVIDSON, M.W. Introduction to Phase Contrast Microscopy. 2016 Nikon Instruments Inc. https://www.microscopyu.com/techniques/phase-contrast/introduction-to-phase-contrast-microscopy.
86. SPRING, K.R. & DAVIDSON, M.W. 2016. Introduction to Fluorescence Microscopy. Nikon Instruments Inc.
https://www.microscopyu.com/techniques/fluorescence/introduction-to-fluorescence-microscopy.

87. NOBEL MEDIA AB. 2017. The Fluorescence Microscope. http://www.nobelprize.org/educational/physics/microscopes/fluorescence/.
88. THERMO FISHER SCIENTIFIC. 2017. Fluorescent probes. https://www.thermofisher.com/no/en/home/life-science/protein-biology /protein-biology-learning-center/protein-biology-resource-library/pierce-protein-methods/fluorescent-probes.html
89. VAHABI, S., SALMAN, B.N. & JAVANMARD, A. 2013. Atomic Force Microscopy Application in Biological Research: A Review Study. Iranian Journal of Medical Sciences 38 (2) p 76-83.
90. LAST, J.A., RUSSEL, P, NEALEY, P.F. & MURPHY, C.J. 2010. The Applications of Atomic Force Microscopy to Vision Science. Investigative Ophthalmology Visual Science, 51(12), p 6083–6094.
91. KURGANSKAYA, I., LUTTGE, A. & BARRON, A.R. 2009. The Application of VSI (Vertical Scanning Interferometry) to the Study of Crystal Surface Processes. http://cnx.org/content/m22326/1.4/
92. ARJMANDI, N. 2013. Resist Homogeneity, Updates in Advanced Lithography, Prof. Sumio Hosaka (Ed.), InTech.
93. SHERMAN, F. 2002.Getting Started with Yeast. Methods Enzymology. Volume 350. p. 3-41

Appendices

A Edge bead measurements

All the measurements made on the resist thickness for master molds number 5 and 8 (prepared as described in table 2.2) are given in table A.1.

Table A.1: Every measurement of the resist thickness made on master molds 5 and 8. The underlined measurement, number 1 for master mold 5 and number 2 for master mold 8, were made at the edge of the wafers.

Measurement #	Resist thickness [μm] Wafer 5	Resist thickness [μm] Wafer 8
1	<u>3,26</u>	2,82
2	2,89	<u>3,25</u>
3	2,91	2,81
4	2,88	2,38
5	2,80	2,87
6	2,88	2,83
7	2,87	2,83
8	2,88	2,90
9	2,88	2,81
10	2,88	2,82